KOCAELI UNIVERSITY
INSTITUTE OF NATURAL AND APPLIED SCIENCES

ELECTRONICS AND COMMUNICATION ENGINEERING DEPARTMENT

MASTER'S THESIS

ENERGY EFFICIENT MASSIVE MIMO DESIGN

MOHAMMED A.A. ABUIBAID

KOCAELI 2018

KOCAELI UNIVERSITY

INSTITUTE OF NATURAL AND APPLIED SCIENCES

ELECTRONICS AND COMMUNICATION ENGINEERING DEPARTMENT

MASTER'S THESIS

ENERGY EFFICIENT MASSIVE MIMO DESIGN

MOHAMMED A.A. ABUIBAID

Asst. Prof. Dr. Sultan ALDIRMAZ ÇOLAK
Supervisor, Kocaeli University .....

Assos. Prof. Dr. Kerem KÜÇÜK
Jury Member, Kocaeli University .....

Asst. Prof. Dr. Köksal HOCAOĞLU
Jury Member, Gebze Technical University .....

Thesis Defense Date: 20.06.2018

ACKNOWLEDGMENTS

I would like to thank the people that I have been working with, who has been supportive and helpful throughout the thesis project, namely:

Professor Sultan Aldırmaz Çolak, my supervisor at Kocaeli University, for providing me with relevant information and inspiration how to tackle different tasks, discussing problems, providing me with useful ideas, and keeping me on track during the research.

M M Aftab Hossain, Post Doc. Researcher at KTH Royal Institute of Technology, for his help by answering questions about problems I faced with MATLAB scripting which was used in the thesis project.

Imad Eid, a senior manager in Wataniya Mobile's Radio network department, for providing me with network statistics analysis and for bringing forward relevant ideas about real network scenarios.

Ayah M.A. Salous, computer engineer at Najah National University, for her help by providing me with algorithm complexity analysis and calculation process simplification.

This research did not receive any specific grant from funding agencies in the public, commercial, or not-for-profit sectors.

June-2018 Mohammed A.A. ABUIBAID

TABLE OF CONTENTS

LIST OF FIGURES

LIST OF TABLES

LIST OF ACRONYMS

AEC	: Average Energy Consumption
BF	: Boundary Focused
BH	: Busy Hour
BS	: Base Station
BW	: Channel Bandwidth
CF	: Center Focused
CSI	: Channel State Information
D2D	: Device-to-Device Communication
DL	: Downlink
DTX	: Discontinuous Transmission
EE	: Energy Efficiency
GDR	: Guaranteed Data Rate
GoS	: Grade of Service
HD	: High Definition
LTE Advanced	: Long Term Evolution Advanced
MF	: Middle Focused
MIMO	: Multi-Input Multi-Output
PA	: Power Amplifiers
PAPR	: Peak to Average Power Ratio
QoS	: Quality of Service
SE	: Spectral Efficiency
SINR	: Signal to Interference and Noise Ratio
TDD	: Time Division Duplex
TPA	: Traditional Power Amplifier
UE	: User Equipment
ULD	: User Location Distribution
VLC	: Visible Light Communication
ZF	: Zero-Forcing

ENERGY EFFICIENT MASSIVE MIMO DESIGN

ABSTRACT

High data rate and energy-efficient design are of paramount importance for 5G systems. Massive multi-input multi-output (MIMO) can ensure both by extending the number of antennas at base station (BS) to a few hundreds and operating in time division duplex (TDD) mode to serve several tens of terminals. This study evaluates the impact of user location distribution (ULD) variation on the energy efficiency of a load-adaptive massive MIMO system. Then, it suggests a dynamic resource allocation strategy that exploits the advantage of ULD variations to attain a more energy-efficient design. Daily ULD variation is modelled by splitting the cell into a certain number of coverage areas and assigning different user densities to each one for each hour. This modelling yields different ULD variations, such as boundary focused (BF), middle focused (MF), uniform, and center focused (CF) ULD variations. For clarity, all cells are assumed identical in terms of BS configurations, cell loading and ULD variation. The simulation performed in this study benchmarks the proposed dynamic strategy with a fixed strategy dimensioned at maximum cell load and BF ULD model. The results show that the optimal number of antennas depends primarily on ULD model and secondarily on cell loading. Up to one third of the active antennas can be turned off daily, and this in turn conserves up to 36-50% of the consumed energy.

Keywords: Energy efficiency, Guaranteed Data Rate (GDR), Massive MIMO, User Location Distribution (ULD) Model.

INTRODUCTION

Next-generation -5G- wireless systems promise to support ultra-high data rate, massive number of connected devices (around 50 billion), very high volume of data transfer, and ultra-low energy consumption. By 2020, these goals are to be actualized through some of these key technology components: multi-antenna transmission (aka massive multi-input multi-output (MIMO)), ultra-lean design, user/control separation, flexible spectrum usage, flexible duplex, direct device-to-device communication (D2D) and access/backhaul integration, spatial modulation, cognitive radio networks, mobile femtocell, and visible light communication (VLC) [1-4].

Massive MIMO can help fifth generation mobile systems to utilize low-cost low-power units operating coherently in the base stations (BSs), where each BS uses a few hundred antennas to serve several tens of single-antenna user equipment (UE) [5-6]. By means of this high ratio of number of BS antennas to number of UEs, a massive MIMO system can deliver higher and more reliable user throughput and achieve better energy efficiency (EE) than typical MIMO systems when interference-suppressing precoding such as zero-forcing (ZF) is utilized [6-10].

The need to minimize operating expenditure (OpEx) and reduce CO_2 emission of the current wireless networks leads the planner of next-generation wireless systems to set EE maximization as one of the design requirements and to define EE metrics to evaluate the greenness of newly proposed techniques. Of particular significance to EE maximization is improving the efficiency of BS (especially power amplifiers (PAs)) since it is responsible for 57% of power usage and 52% of CO_2emission per subscriber per year in a typical mobile network [11-12].

From different points of view, there are several EE metrics to evaluate wireless networks. A well-known metric that is suitable for this study is EE at BS-level, defined as the ratio of total downlink (DL) rate to total power consumption at BS in units of (Mbps/Watt). This metric assesses the energy consumption while considering the capacity of BS and, by considering cell coverage area, can easily be raised to a network-level metric in units of (Mbps/Watt/Km^2), which quantifies the degree of greenness [11-16]. When EE of a massive MIMO system is evaluated by this metric, it can be modelled as a quasi-concave function of three design parameters (K, M, ρ),

namely, number of users K, number of active antennas M, and signal to interference and noise ratio (SINR) ρ. EE maximization is accomplished by an alternating optimization algorithm that uses three closed-form expressions for each one of the design parameters [17].

Improving EE by adaptive resource allocation in wireless BSs that operates with the support of MIMO systems has been studied intensively in previous literature [12-15]. The authors in [12] proposed a technique, named bandwidth expansion, to improve EE at the cost of spectral efficiency (SE) by exploiting the spare bandwidth at low DL traffic conditions and adapting to low-order modulation schemes. In [13], the number of active antennas, which is the same as the number of PAs when each antenna has its own PA, is adapted to cope with daily cell load variation for a multi-cell network with uniform user location distribution (ULD), thereby a significant gain on EE is achieved at low traffic-load states and the gain decreases inverse proportionally to the cell load. In [14], incorporation of discontinuous transmission (DTX) feature, which allows BS to deactivate some of its transmission components during silent traffic periods and reactivate them immediately when traffic is initiated, is examined with beamforming technology for a millimeter wave (mmW) propagation and rural deployment environment with non-uniform ULD. According to the results, DTX feature leads to insignificant EE improvement when beamforming technology is already implemented. In [15], long term evolution advanced (LTE Advanced) systems were considered and their EE was shown to be improved when adopting femtocells and heterogeneous network implementation. These techniques were proposed to cope with non-uniform user location distribution within the network coverage area. However, they do not take into consideration any time-variation in ULD. Assuming ULD is invariant underrates dynamic user behavior, thus rendering a constant EE over time.

In this study, we develop various ULD variations and examines their effects on EE and user-rate of a massive MIMO system. we consider a BS integrated with a massive MIMO system and dimensioned to handle peak DL data traffic at maximum cell loading condition. For this baseline BS, we study EE under different ULD models, namely, boundary focused (BF), uniform and center focused (CF), and investigate EE improvement opportunities. We propose a resource allocation strategy to adapt the number of antennas based on tracking variations of ULD and cell loading on an hourly basis. This strategy is different from [13] by way of its taking advantage of two environment variations to exploit massive MIMO favorable propagation and to lower

the number of active antennas while maintaining a tolerable user-rate loss and thus operating more efficiently.

For fairness, we compare our simulation results with a fixed antenna system dimensioned with the same network conditions. When cell loading varies between 10% and 100%, the proposed strategy results in 47%, 113% and 222% average EE gain at the cost of 19%, 35% and 35% average user-rate loss over fixed antenna massive MIMO system for BF, uniform and CF ULD models, respectively. In addition, when center-to-boundary user ratio changes from 90/10% (CF) to 10/90% (BF), the strategy can improve user-rate by a factor of two at the boundary area and by a factor of one and a half at the center area. On daily basis, the strategy can turn off up to one third of the fixed antenna system, thereby saving 36%-50% of the daily-consumed energy.

The remainder of this study is organized as follows[1]: Section 0 describes the models and assumptions used for simulation and Section 0 tackles the EE maximization problem. Then, we discuss the simulation results in Section 3 and conclude the study in Section 0.

[1]Upper-case plain symbols represent matrices while lower-case fonts denote scalar variables.

1.MODELS AND ASSUMPTIONS

1.1. Massive MIMO System Model

In this study, we consider a DL of a multi-cell massive MIMO system that contains N hexagonal cells, where each cell $BS_i \in N$ consists of one BS placed at the cell center and is equipped with M_i antenna elements that communicate with K_i single-antenna users, such that $M_i > K_i$. The users are distributed inside each cell according to ULD models given in Section 1.2. Each BS transmits a constant output power P_c that is distributed equally among PAs, where each PA is connected to one antenna element. Thus, the mean output transmission power per antenna is $p = P_c/M_i$. We assume that all BSs and UEs are synchronized and operate on time-division duplex (TDD) protocol. In addition, all BSs employ ZF precoding to cancel out intra-cell interference by using beamforming technique and can perfectly estimate channel state information (CSI) of UEs by using the uplink pilots sent by UEs at the first part of transmission blocks.

We assume antenna array elements are adequately spaced apart such that the channel components at UE_z are uncorrelated and the path distances are the same since the distances to UE_z are much greater than the distance between array elements, where UE_z denotes a UE at location z. The channel is assumed to be a block flat Rayleigh channel and to remain static within a time-frequency coherence block of T_cB_c symbols, where B_c is the coherence bandwidth in Hz and T_c is the coherence time in seconds. Assuming the channel response is a realization of a zero-mean circularly symmetric complex Gaussian distribution, the channel response $h_{jiz} \in C^M$ between BS_j and UE_z in cell BS_i within a transmission block is such that

$$h_{jiz} \sim CN\left(0, d_j(UE_z) I_{M_j}\right) \tag{1.1}$$

In Eq.(1.1), I_{M_j} is an $M_j \times M_j$ identity matrix, $d_j(UE_z)$ is a deterministic function that accounts for large scale fading (i.e., channel attenuation due to path loss shadowing and scattering) between BS_j and UE_z in cell BS_i. Built on above assumptions, the distance-dependent rate at UE_z within cell BS_i can be found by [13]:

$$R_{UE_z}(K_i)= B\left(1-\frac{\alpha K_{max}}{T_c B_c}\right)\log_2\left(1+\frac{p\frac{M_i}{K_i}(M_i- K_i)}{\frac{B\sigma^2}{d_i(UE_z)}+ \sum_{j=1}^{J}\left\{\frac{d_j(UE_z)}{d_i(UE_z)}\ p\ M_j\right\}}\right) \quad (1.2)$$

where B is the effective channel bandwidth (BW), α is the pilot reuse factor, K_{max} is the maximum number of users that can be served simultaneously, which is assumed to be the same for all cells, αK_{max} is the number of pilot sequences, $T_c B_c$ is the length of the channel coherence block interval as mentioned before, and $B\sigma^2$ is total noise power. Note that the pre-log factor $\left(1-\frac{\alpha K_{max}}{T_c B_c}\right)$ accounts for rate loss due to necessary overhead for channel estimation. The term $d_i(UE_z)$ represents the path loss from the serving BS at origin cell BS_i to UE_z and the term $d_j(UE_z)$ represents the path loss from interfering cell BS_j to UE_z inside the origin cell BS_i. These terms depend on the simulation environment parameters such as cell radius, cell shape, tier size, i.e., the number of neighbors, and ULD model. Looking inside the logarithm, $\frac{B\sigma^2}{d_i(UE_z)}$ accounts for the average noise power that disturbs the received signal from the serving BS, $\sum_{j=1}^{J}\left\{\frac{d_j(UE_z)}{d_i(UE_z)}\ p\ M_j\right\}$ accounts for the average interference power from all neighbor interfering cells, where J is the number of neighbor interfering cells. The term $p\frac{M_c}{K_c}$ represents the mean transmit power per user, and the ratio $(p\frac{M_i}{K_i})/\sum_{j=1}^{J}\left\{\frac{d_j(UE_z)}{d_i(UE_z)}\ p\ M_j\right\}$ is proportional to the SINR, and$(M_i- K_i)$ is the array gain of massive MIMO. Note that the BS handles a sum rate of $\sum_{k=1}^{K_{max}} R_{UE_z}(k)$.

1.2. Modeling ULD

People want to feel free to consume data in transit as in household. Increasing traffic congestion means people spends more time in cars; thereby more in-car mobile data demand to access information, social networks, and entertainment music and video services. Apart from that, driver assistance systems, usage-based insurance, navigation and real-time traffic status facilitate vehicles driving and make it more secure and comfortable. However, being connected is not the only requirement for future mobile services but also perceiving adequate quality of experience through civilian various time allocations in Figure 1.1. As a result, dimensioning mobile services demand based on user locations ultimately drive operators' investments.

User location density and user mobility models are two key factors behind modelling ULD. For example, the land geographical features, such as coastlines, hilly lands, lakes, rivers, etc., and places with high population density (i.e., workplaces, highways, apartment complexes, stadiums, malls) both aggregate the users in confined areas and limit their mobility into specific patterns.

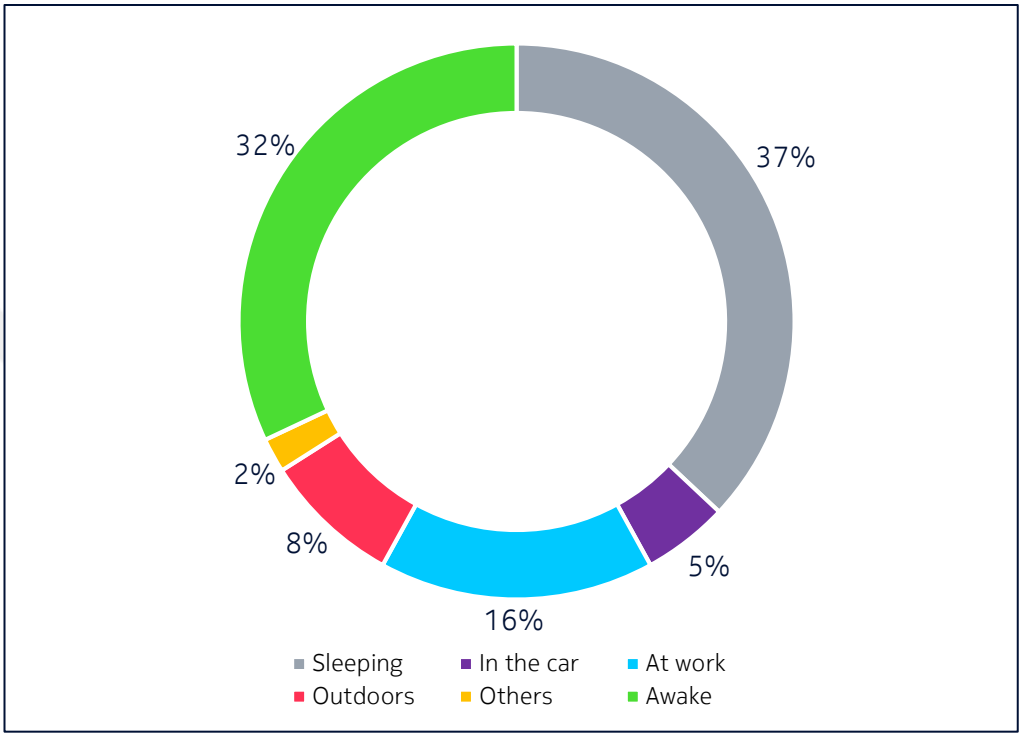

Figure 1.1. The average civilian time allocation [18]

In this work, ULD model defines a set of areas formed by a set of radii $\delta = \{\delta_1, \delta_2, \ldots, \delta_q\}$, where $\delta_1 > \delta_{min}$, $\delta_q < \delta_{max}$ and assigned a set of weighting factors $\gamma = \{\gamma_1, \gamma_2, \ldots, \gamma_q, \gamma_{q+1}\}$. Each weighting factor is a function of time so that it can take different values during the day. However, the sum of weighting factors at any time instant t is always unity, i.e. $\sum \gamma = 1$. The following symmetric example is used for simulations.

Example 2.1. Suppose cell BS_i is split up into three coverage areas by $\delta_i = \{\delta_1, \delta_2\}$ and these areas are assigned a set of weighting factors $\gamma_i = \{\gamma_c, \gamma_m, \gamma_b\}$. Determine when ULD model takes the forms CF, middle focused (MF), BF and uniform.

User density at each ring in cell BS_i can be expressed as follows:

$$U_i=\{u_c\ ,\ u_m,u_b\}=\left\{\frac{\gamma_c\ K_{max}}{A_c}\ ,\ \frac{\gamma_m\ K_{max}}{A_m},\ \frac{\gamma_b\ K_{max}}{A_b}\right\} \tag{1.3}$$

where $A_c=\pi(\delta_1^{\,2}-\delta_{min}^{\,2})$, $A_m=\pi(\delta_2^{\,2}-\delta_1^{\,2})$ and $A_b=3\sqrt{3}\,\delta_{max}^{\,2}/2-\pi\delta_2^{\,2}$ are the areas of center, middle and boundary regions, respectively. The form of ULD is determined by the maximum value of user density set U_i as follows:

$$\max U_i=\begin{cases} u_c\ , & \text{Center-Focused} \\ u_m\ , & \text{Middle-Focused} \\ u_b\ , & \text{Boundary-Focused} \\ \emptyset\ , & \text{Uniform Distribution} \end{cases} \tag{1.4}$$

Note that when user densities are equal for all areas, ULD takes the form of uniform distribution. Figure 1.2 shows how cell BS_i is divided up into three areas each with its own user density, U_i.

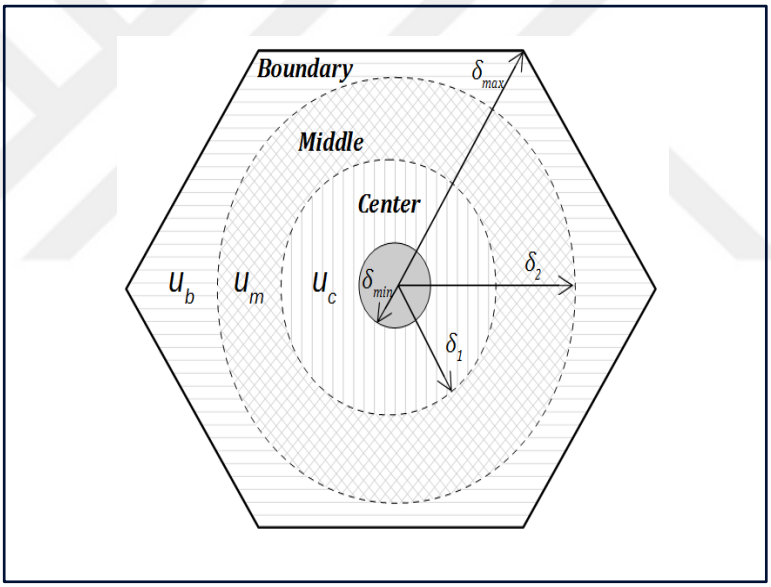

Figure 1.2. Cell coverage area split into center, middle, and boundary regions

To capture the ULD variation on hourly basis, we assume a daily user mobility pattern as illustrated in Figure 1.3. At night hours, the users generally show stationary behavior in residential areas which we call 1st aggregation area. In the morning, the users move to a 2nd aggregation area, such as workplace or campus area, and stay there for some hours.

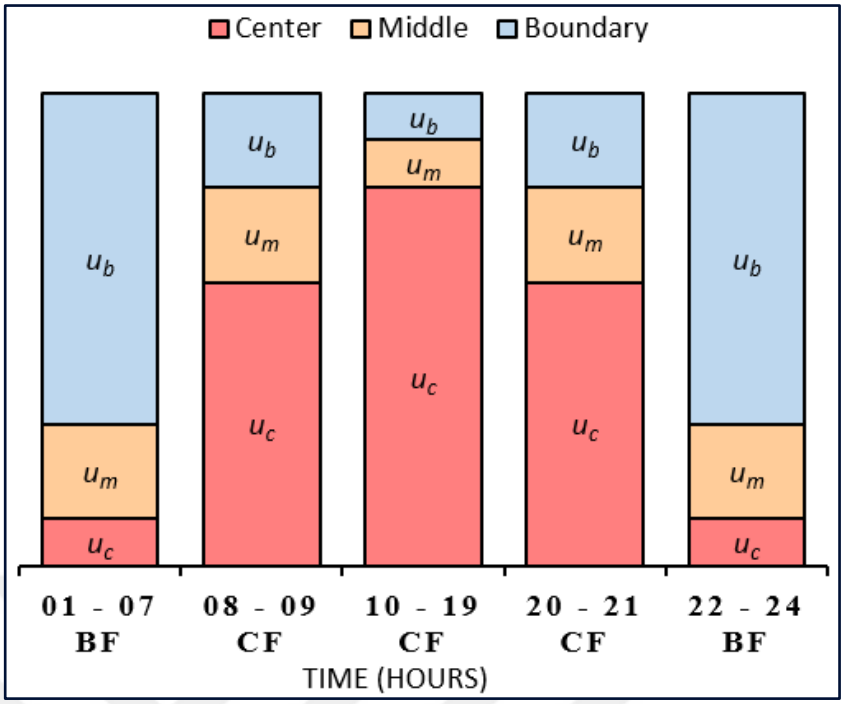

(a)

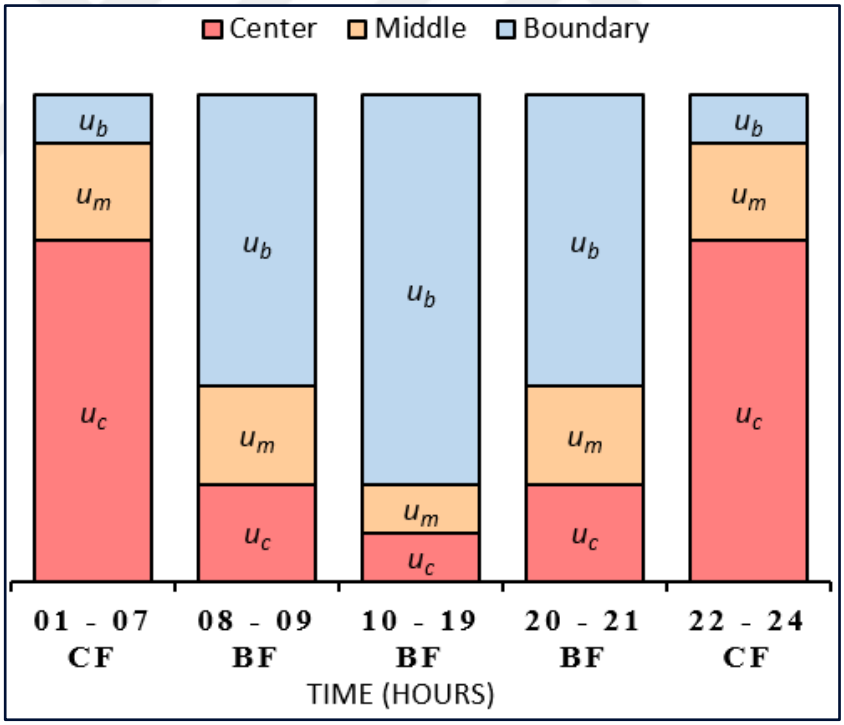

(b)

Figure 1.3. Daily ULD scenarios a) Daily ULD variation characterized as BF, CF then BF b) Daily ULD variation characterized as CF, BF then CF

In the evening, they return to the 1st aggregation area and the same behavior repeats at night. If the BS of the cell under study is closer to the 2nd aggregation area than the

1st one, then the daily ULD variation is characterized as BF, CF and lastly BF as shown in Figure 1.3 (a). On the contrary, the daily ULD variation is characterized as CF, BF then CF as shown in Figure 1.3 (b) when the BS is closer to the 1st aggregation area than the 2nd one.

1.3. Data Traffic Demand

Providing high speed connectivity is of high importance for mobile operators to score high user satisfaction. For this aim, mobile network resources are not dimensioned to account data traffic volume only but also to the type of connected devices, category of installed mobile application, average time users spend on mobiles.

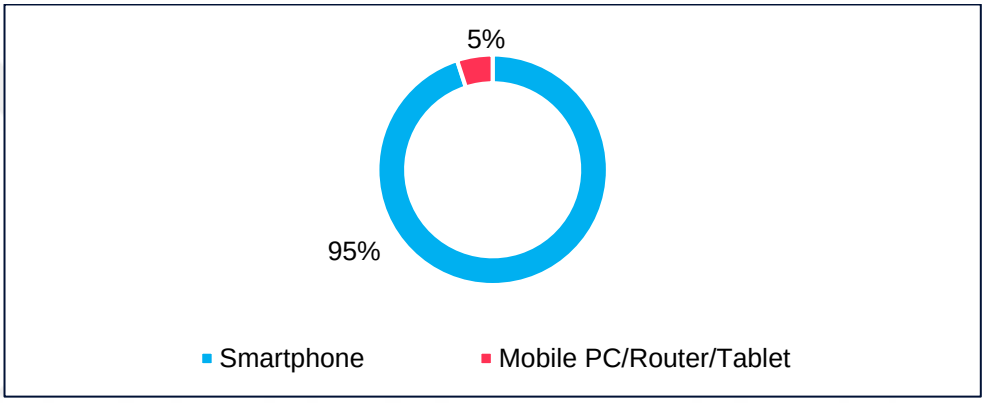

(a)

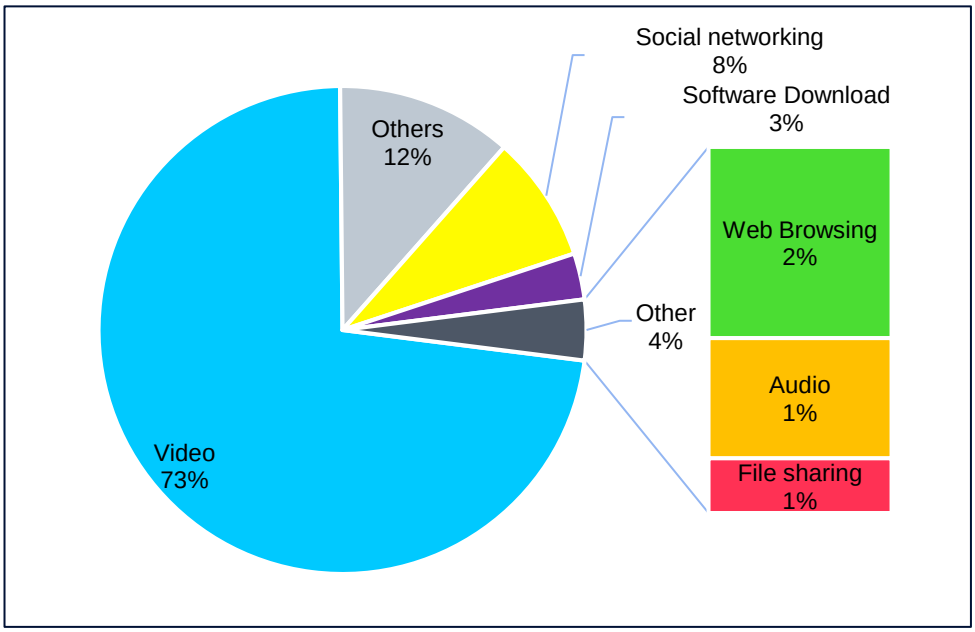

(b)

Figure 1.4. Ericsson world-wide mobile data traffic forecast [20] a) Split per device category b) Split per application category

Presenting to Ericsson 2023 mobile date traffic forecast as shown in Figure 1.4, smartphones are anticipated to consume 94% of future date traffic while 4% contribution comes from others connected devices like mobile PCs, routers and tablets. Due to trends of new video formats such as 360-degree videos and users' tendency to watch high definition (HD) 1080p and 720p videos, mobile video streaming gets the lion's share at 73% of total traffic demand. According to Huawei Wireless X Labs, people will spend on mobile devices 3.5 hours and 5.5 hours per day by 2020 and 2025, respectively [22]. We adapt Eq.(1.5) from [18] for translating data traffic demand into BS date-rate as follows:

$$R_{BS}=K_{max}\sum_{i}\sum_{j}\sum_{k}\frac{1024^3\times 8\times G_i\times X_i\times D_j}{30\times 24\times A_F\times 60^2\times 10^6} \tag{1.5}$$

where K_{max} is number of connected users at busy hour (BH), 1024^3 is Bytes per GB, 8 is bits per byte, G_i and X_i are the monthly data traffic demand in GB and the total traffic share of application category i, respectively, D_j is the ratio of users of device category j , 30 is days per month, 24 is hours per day, A_F is activity factor defined as average time ratio users spend on mobile devices, 60^2 is seconds per hour, 10^6 is bits per Mb.

1.4.Daily Data Traffic Load Model

In [22], Nokia Bell-Labs maps all upcoming mobile services into five application categories: streaming, computing, gaming, communication and storage applications. For example, audios and videos belong to streaming application category, web services and application management lie under computing category, cloud-based backup and device-sync services are linked to storage application category. Communication application category includes services like voice over internet protocol (VoIP), video calls, instant messaging, emails and internet of things (IoT). The daily traffic demand variation of each application category results various daily BS loads. As shown in Figure 1.5, the peak BS load for storage applications is around 6:00 AM, while for communication and computing applications around 12:00 PM and 04:00 PM, respectively, and for streaming and gaming applications around 09:00 PM and 10:00 PM, respectively. For sake of simplicity, in this study we assume BS load varies according to streaming application category only. However, same analysis can be carried out for other application categories.

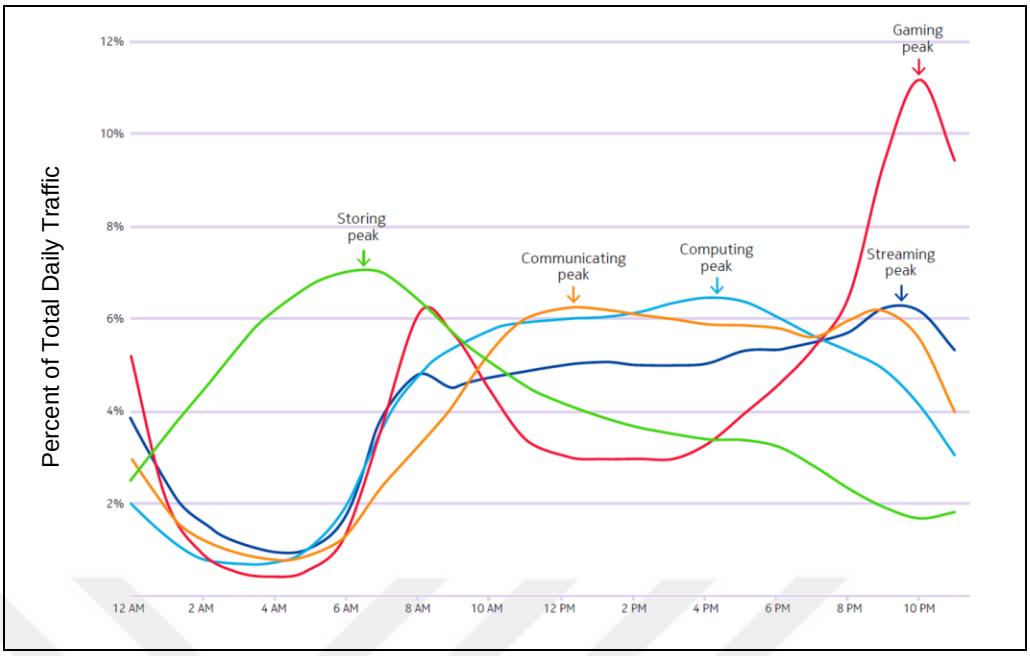

Figure 1.5. Daily traffic distribution for 5 categories of mobile applications [22]

In accordance to BS load variation, the number of active users varies at each time instant t. To capture and link both variations, we model the BS of cell under study as an M/G/m/m state dependent queue where users arrive according to a Poisson process with rate λ and treated in order of arrival. Users' service times are independent and identically distributed with some general distribution function. Each cell BS_i has m servers available and every newly arriving user immediately goes into service if there is a server available, and that user is lost if all servers are occupied. The steady state probability distribution of having k users at a time instance t, $\pi_i(k,s_t)$, is given by Eq. (1.6.a)

$$\pi_i(k,s_t)=\left[\frac{\left[\lambda_{max}\frac{s_t}{R_{UE_z}(1)}\right]^k}{k!f(k)f(k-1)\dots f(2)f(1)}\right]\pi_i(0,s_t) \quad (1.6.a)$$

$$\pi_i^{-1}(0,s_t)=1+\sum_{m=1}^{K_{max}}\left(\frac{\left[\lambda_{max}\frac{s_t}{R_{UE_z}(1)}\right]^m}{m!f(m)f(m-1)\dots f(2)f(1)}\right) \quad (1.6.b)$$

In Eq. (2.6) λ_{max} is the maximum user arrival rate, s_t is the average data volume contribution by a single user at time instance t, $f(k)=R_{UE_z}(k)/R_{UE_z}(1)$ is the rate at user state k normalized by user state 1, i.e. when BS serves a single user, $\pi_{BS_i}(0,s_t)$ is the

probability of BS_i having no users, the number of servers in the queue is the same as the number of users and, lastly, K_{max} is the maximum number of users the queue can serve, as will be derived in Section 2.1. The M/G/m/m queue is assumed to have a certain grade-of service (GoS) that corresponds to the blocking probability while serving the maximum number of users K_{max} at peak cell loading. The probabilities for other states can be derived by assuming $\lambda_{max}= K_{max}$ and finding the maximum value of s_t, s_{max}, that is associated with $\pi_{BS_i}(K_{max}, s_{max})$=GoS. Then the value of $\pi_{BS_i}(k, s_{max})$ can be obtained for k=1,2,.., K_{max}. To calculate user steady state probabilities at different cell load conditions, we just need to use $s_t= s_{max}/x_t$, where x_t is the cell loading at time instant t. Note that $R_{UE_z}(k)$ for the above calculations is found using Eq. (1.2). Due to the requirements of transmitting cell information and connection control and management signaling, it is assumed that the minimum cell load is 10% [19]. User steady state probabilities at minimum, half and peak cell loadings; i.e. 10%, 50% and 100%, respectively, are shown in Figure 1.6.

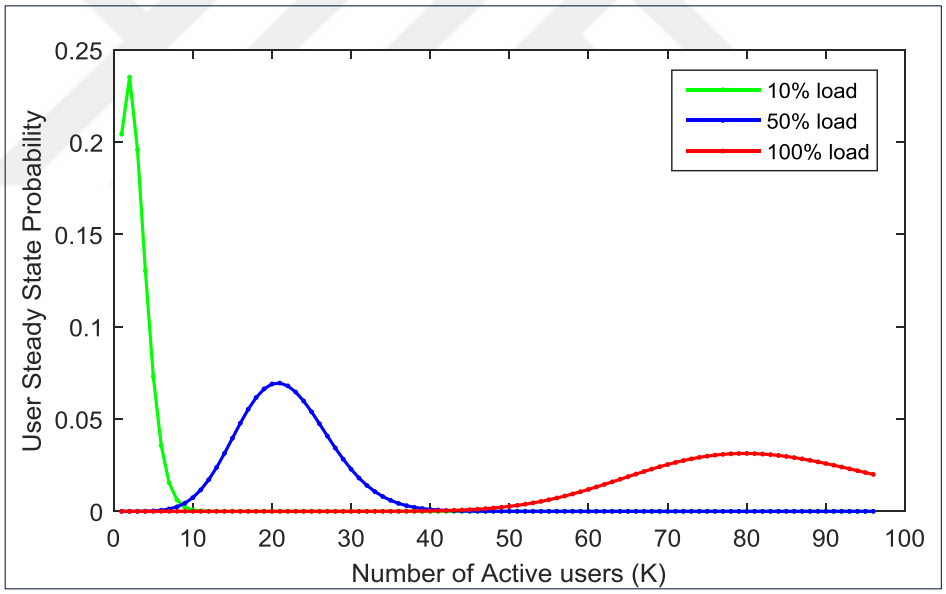

Figure 1.6. User steady state probabilities at 10%, 50% and 100% loadings

1.5. BS Power Consumption Model

The circuit power consumption model proposed in [17] gives realistic relations between the total consumed power at BS and the important dimensioning parameters (M, K, R_{UE_z}). It also considers the dynamic efficiency characteristics of realistic PAs. In accordance with this model, the total DL baseband power can be approximated as:

$$P_{total} \approx C_0 + C_1 M_i \tag{1.7.a}$$

$$C_0 = \sum_{k=1}^{K_{max}} R_{UE_z}(k)\,(P_{COD} + P_{DEC}) + P_{SYN} + \frac{BK_i^3}{3T_c B_c L_{BS}} + P_{oth} \tag{1.7.b}$$

$$C_1 = P_{BS} + \frac{BK_i\,(2 + (T_c B_c)^{-1})}{L_{BS}} + \frac{3B\,K_i^2}{L_{BS}} + P_{PA}(p) \tag{1.7.c}$$

where $\sum_{k=1}^{K_{max}} R_{UE_z}(k)$ is the total rate handled by the cell BS_i as calculated in Eq. (1.2), P_{COD} and P_{DEC} are the power required for coding and decoding, respectively. P_{SYN} is the power consumed by the local oscillator, L_{BS} is cell BS_i computational efficiency, $P_{PA}(p)$ is the total input power required for mean output transmission power p of a traditional power amplifier (TPA) as given in [24-26]:

$$P_{PA}(p) \approx \eta^{-1} \sqrt{p \cdot P_{max,\,PA}} \tag{1.8}$$

where η is the maximum TPA efficiency, $P_{max,PA}$ is the maximum output transmission power. Since the peak to average power ratio (PAPR) in latest technologies is around 8 dB, $P_{max,PA}$ should be higher than the maximum mean output transmission power p_{max} at most by that amount. Another important absolute measure of energy to compare how much saving can be attained for one day is the average energy consumption (AEC) per BS coverage area expressed in units of kWh/km^2 as follows:

$$AEC_{BS} = \sum_{t=1}^{24} \frac{P_{total}(t) \times 60 \times 60}{24 \times \text{Coverage Area}} \tag{1.9}$$

2.PROBLEM FORMULATION

The EE (Mbit/Joule) is defined as system throughput per unit of energy consumption [16]. Accordingly, EE at BS-level is calculated as the ratio of sum rate handled by BS (Mbit/s) to the total consumed power (Joule/s). Now, by using Eq. (1.2) and Eq. (1.7), EE can be expressed as:

$$EE_i = \frac{\text{Sum Rate}}{\text{Total Consumed Power}} = \frac{\sum_{k=1}^{K_{max}} R_{UE_z}(k, M_i , M_j)}{P_{total}(M_i , K_i)} \tag{2.1}$$

As Eq. (2.1) shows, the achieved EE at cell BS_i depends not only on its own number of antennas but also on the number of antennas of other interfering BSs. That is, the EE formula accounts for the asymmetrical multi-cell environment, which in turn forms an intractable joint optimization problem. To facilitate EE maximization analysis, we assume that the multi-cell environment is symmetrical in terms of cell loading, ULD model and BS configurations. Built on these assumptions, the number of antennas for all cells will be the same so that Eq. (2.1) can be simplified by setting $M_j = M_i$ to become:

$$EE_i = \frac{\sum_{k=1}^{K_{max}} R_{UE_z}(k, M_i)}{P_{total}(M_i , K_i)} \tag{2.2}$$

Now, the optimal number of antennas for all user states, M_{opt}, can be found by maximizing EE for a certain ULD model formed as below:

$$M_{opt}(k) = \arg\max_{M_i} \frac{\sum_{k=1}^{K_{max}} R_{UE_z}(k, M_i)}{P_{total}(M_i , K_i)} \tag{2.3}$$

$$\text{Subject to: } M_i \geq \left\lceil \frac{P_c}{P_{max,PA}} 10^{0.8} \right\rceil, M_i \geq k + 1$$

In Eq.(2.3), the first constraint sets the minimum number of antennas by keeping PAPR of the transmitted signal at 8 dB. The second one comes from applying ZF precoding technique at the BS. A weighted-average value of M_{opt} at a certain cell loading condition x_t can be calculated as:

$$M_{avg}^{(t)} = \left\lceil \sum_{k=1}^{K_{max}} \pi_{BS_i}(k, s_{max}/x_t) \cdot M_{opt}(k) \right\rceil \quad (2.4)$$

As a rule of thumb, systems should be dimensioned at most critical conditions. For this study, operating on maximum cell loading and BF ULD is the most challenging case. Therefore, to cope with this case, we start by dimensioning a fixed antenna system operating at the most energy-efficient values of M and K. By using Eq. (2.2) within a reasonable range of M and K, we search for the number of antennas and users that yield maximum EE. Let us denote these reference values by (K_{max}, M_{max}). The fixed antenna system operates M_{max} antennas whatever changes occur in cell loading, number of active users or ULD model. As stated in Sections 1.2 and 1.4, the ULD model and cell load fluctuate all the time. For this reason, adopting any fixed resource allocation technique will be inefficient in terms of EE. Therefore, we seek a dynamic resource allocation strategy to attain a more energy-efficient massive MIMO design.

2.1. Optimum Number of Antennas for Maximum EE Algorithm

We propose an EE optimization strategy that tackles the users varying behaviors and allocates BS resources adaptably. The strategy runs an algorithm to find the optimal number of antennas that matches the instantaneous system conditions: cell loading, ULD model, and the number of active users. The algorithm starts by setting the number of antennas at all BSs, M_i, to M_{max} which is the value designed for the fixed antenna system. Then, it iteratively updates M_i by the weighted-average optimal number of antennas, M_{avg}, for the cell under study until its value converges. At this point, the optimal number of antennas, M_{opt}, corresponding to all user states is identical for all cells. Note that the iterations are carried out only for the cell under study since all cells are assumed symmetrical in all configurations. The parameters, initialization and computation of the proposed strategy are outlined in Figure 2.1. The EE in Eq. (2.2) represents a quasi-concave function of the number of users and the number of antennas but currently there is no closed form expression for optimal number of antennas, M_{opt}, that maximizes EE at each user's state, k. However, since M_i and k are integer values, the algorithm searches extensively for M_i that maximizes EE over each user state using Eq.(2.3). As can be noted, this step is computationally the most expensive part in the algorithm. Therefore, the algorithm's time complexity can be approximated to the order of $O(n^2)$, where n^2 denotes size of $M_i \times k$ matrix.

Obtaining M_{opt} by a more time-efficient way is beyond the scope of this thesis and hence left for future work.

Initialization:

$M_{avg} \leftarrow M_{max}$

Computation:

do {

$M_i \leftarrow M_{avg}$

for all users' states $k \in [1, K_{max}]$ do

$$M_{opt}(k) \leftarrow \underset{M_i}{\arg\max:} \frac{\sum_k R(k, M_i)}{P_{total}(M_i, K_i)}$$

subject to: $M_i \geq M_{min}, M_i \geq k + 1$

end for

$$M_{avg} \leftarrow \left\lfloor \sum_{k=1}^{K_{max}} \pi_{BS_i}(k, s_t) \cdot M_{opt}(k) \right\rfloor$$

}

while ($M_j \neq M_{avg}$)

Figure 2.1. Adaptive antenna system at maximum EE Algorithm

2.2. Optimal Number of Antennas for Guaranteed QoS Requirements

In this study, we propose two criteria to master the quality of service (QoS) and improve the user-rate loss results in EE optimization Figure 2.1. First, maintaining a minimum amount of average user-rate on BS level, R_{BS}. Second, assuring a ratio of users (Q_{UE}) getting a guaranteed amount of data rate. In both criteria, the BS resources i.e. optimal number of antennas, M_{opt}, are upscaled gradually as shown in Figure 2.2 until the QoS requirements are fulfilled. In the 1st criteria, the optimal weighted-average user-rate, R_{opt} is dimensioned to approach the guaranteed BS average user-rate, i.e. R_{BS}, which is also can be used as a performance metric to evaluate overall DL speed. In contract, the 2nd criteria improve DL date rate from user prospective. It starts by finding the percent of users getting data rate higher than a minimum guaranteed data rate, Q_{opt}, results from Figure 2.1. Then, it employs more BS antennas until percent of users satisfying guaranteed date rate reached i.e. Q_{UE}. Note that all dimensioned values in Figure 2.1. are prerequisites to start both criteria in Figure 2.2.

.Initialization:

Run Algorithm {Figure 2.1}

$R_{opt} \leftarrow \left\lfloor \sum_{k=1}^{K_{max}} \pi_{BS_i}(k, s_t) \cdot R\left(k, M_{opt}(k)\right) \right\rfloor$

$R_{BS} \leftarrow R_{BS,min}$

Computation:

while ($R_{opt} < R_{BS}$)

do {

for all users' states $k \in [1, K_{max}]$ do

$M_{opt}(k) \leftarrow M_{opt}(k) + c_i$ subject to: $M_{opt} \leq M_{max}$

end for

$R_{opt} \leftarrow \left\lfloor \sum_{k=1}^{K_{max}} \pi_{BS_i}(k, s_t) \cdot R\left(k, M_{opt}(k)\right) \right\rfloor$

}

(a)

Initialization:

Run Algorithm {Figure 2.1}

$R_{UE} \leftarrow R_{UE,min}$

$Q_{UE} \leftarrow Q_{UE,min}$

$Q_{opt} \leftarrow \left\lceil \frac{\sum_{i=1}^{K_{max}} k_i}{K_{max}} \right\rceil$ subject to: $R\left(k_i, M_{opt}(k_i)\right) \geq R_{UE}$

Computation:

while ($Q_{opt} < Q_{UE}$)

do {

for all users' states $k \in [1, K_{max}]$ do

$M_{opt}(k) \leftarrow M_{opt}(k) + c_i$ subject to: $M_{opt} \leq M_{max}$

end for

$Q_{opt} \leftarrow \left\lceil \frac{\sum_{i=1}^{K_{max}} k_i}{K_{max}} \right\rceil$ subject to: $R\left(k_i, M_{opt}(k_i)\right) \geq R_{UE}$

}

(b)

Figure 2.2. Adaptive antenna system with guaranteed QoS Algorithms a) Guaranteed Average User-rate at BS b) Guaranteed percent of users satisfying certain data rate

2.3. Algorithms Complexity Analysis

Considering the user-rate is proportional to the number of BS antennas and $R(k, M_{opt}) < R_{BS|UE} < R(k, M_{max})$ enable us to adopt some root-finding methods; thereby; lower number of iterations. In this work we use interval-halving method i to update $M_{opt}(k)$ by variable step size c_i. It considerably leads to a high-speed processing and time-efficient calculation.

3. NUMERICAL ANALYSIS

In this work, the simulation environment consists of 19 hexagonal cells as illustrated in Figure 3.1, where the pilot reuse factor is set to 1/1. Using Monte-Carlo insertion method, we distribute 10000 test points in the area bounded between the circle of radius δ_{min}=35m and the cell edge according to ULD models formed by sets δ and γ as specified in Section 1.2. The path distance from each interfering BS to each test point is calculated according to the wrap-around algorithm that helps us discard boundary effects when the interfering BS is out of the first tier of neighboring BSs [24]. For clarity, we assume all cells are symmetrical in ULD and cell loading variations, as well as BS configurations. That is, all cells will experience the same level of interfering power at any time instance t. Under those circumstances and using the parameters shown in Table 1, some of which are taken from [13] and [17], we carried out the analysis until it reached convergence point, where all cells have the same optimal average number of antennas.

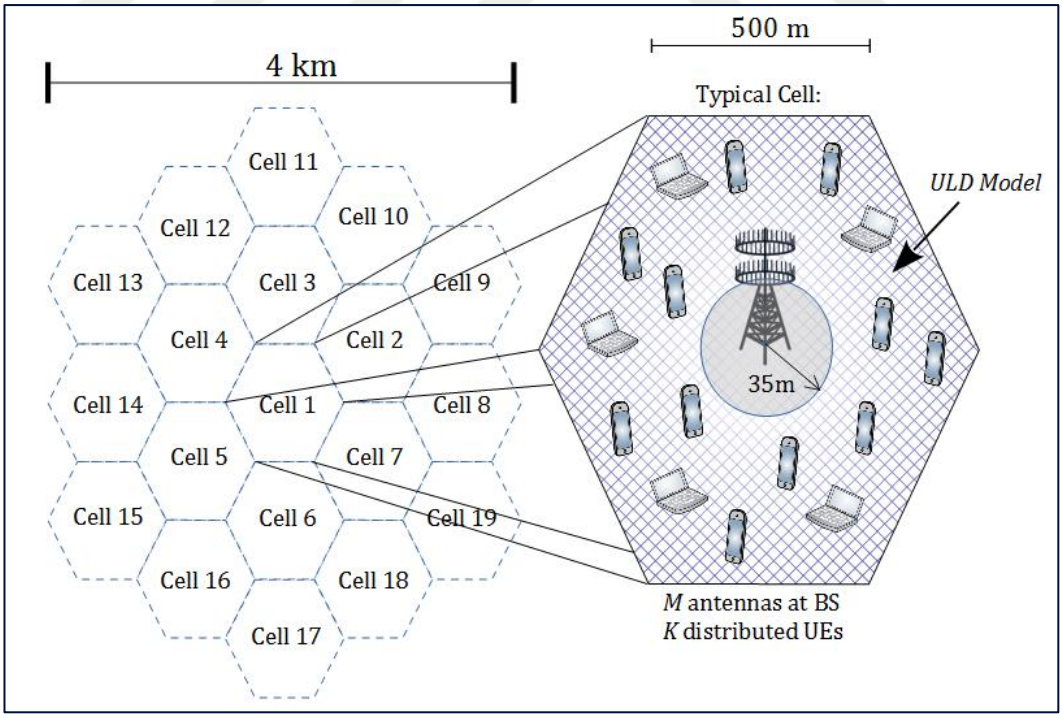

Figure 3.1. Network coverage area where cell under study is surrounded by 18 identical cells

Table 3.1. Network simulation parameters

Reference Parameters	
Parameter	Value
Number of cells	19
Number of test points	10000
Cell Radius: δ_{max}	500 m
Minimum distance: δ_{min}	35 m
Bandwidth	20 MHz
Total noise power: $B\sigma^2$	-96 dBm
Path loss model	$10^{-3.53}/\|\|d\|\|^{3.76}$
Channel coherence time: T_c	10 ms
Channel coherence BW: B_c	180 kHz
Coherence Block: T_cB_c	1800 symbols
BS average transmit power	20 W
Maximum PA efficiency: η	80%
PA maximum output transmission power: $P_{max,\ PA}$	6 dB
Local oscillator power: P_{SYN}	2 W
BS circuit power: P_{BS}	1 W
Other power: P_{oth}	18 W
Power for data coding: P_{COD}	0.1 W/(Gbit/s)
Power for data decoding: P_{DEC}	0.8 W/(Gbit/s)
Power for backhaul traffic: P_{BT}	0.25 W/(Gbit/s)
Computational efficiency at BSs: L_{BS}	12.8 Gflops / W
M/G/m/m queue GoS:	0.2%

Table 3.2. Illustration of CF, Uniform and BF ULD models

ULD Model				
	(c) BF ULD	Weighting Factors	γ_{BF}={0.1, 0.2, 0.7}	δ={200, 400} m
		Set of Radii		
	(b) Uniform ULD	Weighting Factors	γ_{Uni}={0.2, 0.6, 0.2}	δ={200, 400} m
		Set of Radii		
	(a) CF ULD	Weighting Factors	γ_{CF}={0.8, 0.1, 0.1}	δ={200, 400} m
		Set of Radii		

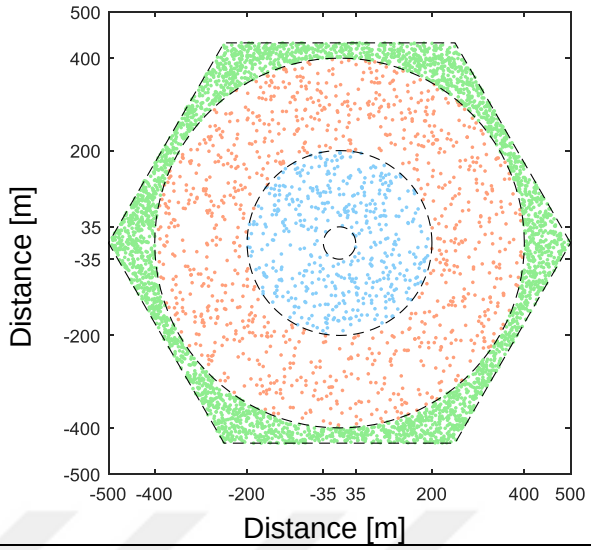

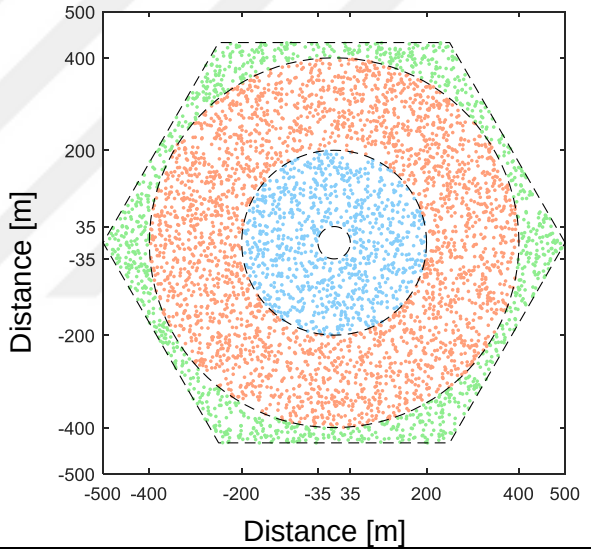

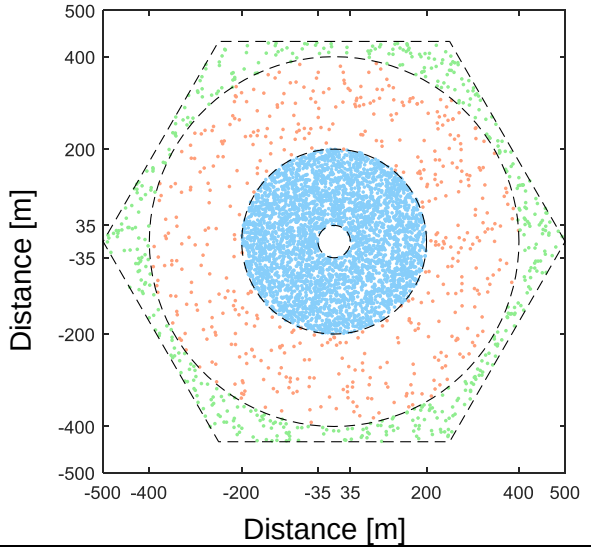

3.1.Optimum Number of Antennas for Maximum EE

To study the effects of different ULD models on optimal number of antenna allocation, we form three ULD models, namely, BF, Uniform, and CF, by dividing the cell into three coverage areas and employing the sets shown in Table 3.2. Then, we run the proposed strategy in Section 2.1 to determine the optimal number of antennas, M_{opt}, for each ULD model at 10%, 50% and 100% cell loading conditions. The relation between M_{opt} and the number of active users, K_i, is almost linear and depends on the ULD model and cell loading simultaneously. Indeed, ULD model provides a major contribution in determining M_{opt} while cell loading provides a minor one. However, the role of cell loading variation decreases dramatically as the ULD model moves from BF to CF distribution.

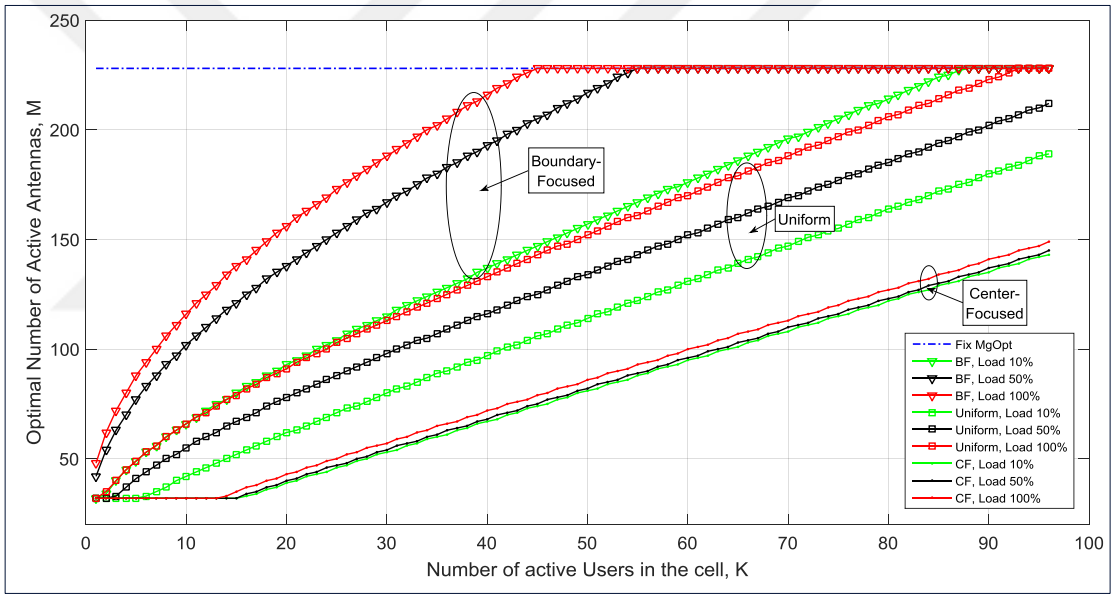

Figure 3.2. Relation between number of antennas (M) and number of users (K) for BF, uniform and CF ULD models at 10%, 50% and 100% cell loadings

Note that the optimal number of antennas has an upper bound, M_{max} and a lower bound M_{min}. As found in Section 2.1, the upper bound is 228 antennas, which is used to operate the baseline fixed antenna system without considering any variations of cell loading, ULD model, or number of active users. The lower bound arises from two limitations. The first one is that each BS radiates at a fixed average transmission power P_c=20 W and distributes this power equally among all antennas. The second limitation is that the PAPR of the transmitted signal must be around 8 dB, which compels the PAs to operate within mean output transmission power $0.087 \leq p \leq 0.630$. Complying with these conditions, the lower bound of the optimal number of antennas

is set to [20/0.630]=32 antennas. The effects of different ULD models on the allocation of optimal number of antennas for all user states at minimum, half and peak cell loadings are illustrated in Figure 3.2.

3.2. Adaptive Versus Fixed Antenna Systems

To evaluate the pros and cons of adaptive and fixed antenna allocation strategies, we examine their average number of antennas, EE, and user-rates on ULD models illustrated in Table 3.1. The fixed antenna system represents a conventional BS puts all antennas in operation regardless of any change in ULD or network loading. Number of antennas in fixed systems is planned to cope with peak BS load on BF ULD model. i.e. busy-hour traffic and poorest radio conditions.

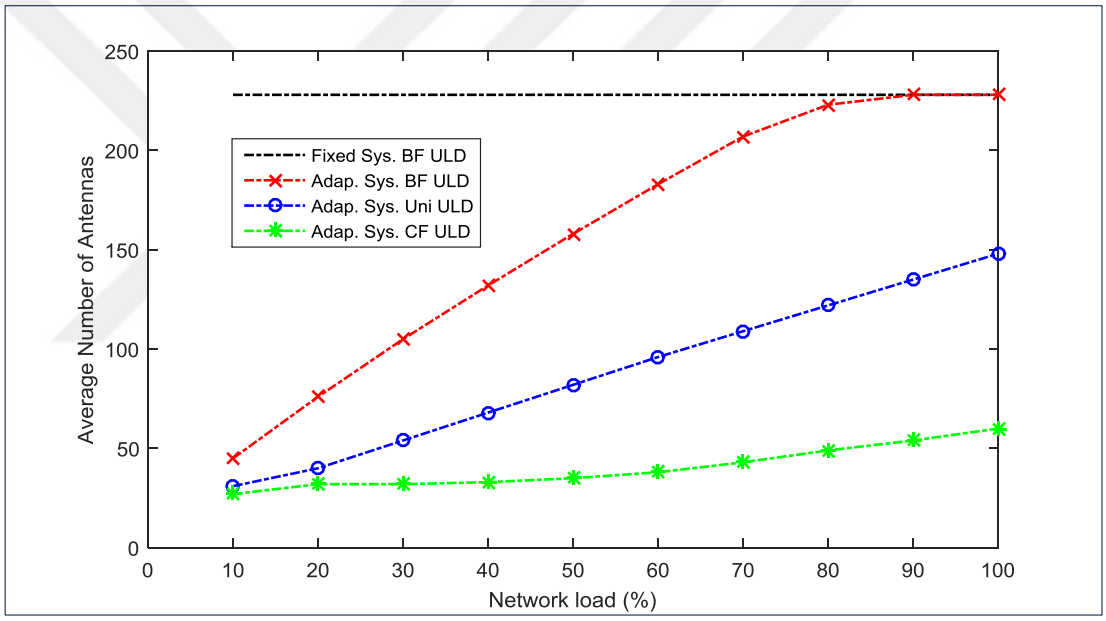

Figure 3.3. Number of antennas of fixed and adaptive systems

As can be seen in Figure 3.3, fixed system has a constant number of antennas (in black dot-slash line) over all network loadings and it's reached only by adaptive antenna system on BF ULD model at 100% network load. Adaptive antenna system reacts differently against network loading in accordance to ULD model. It operates around 2.15, 1.33 and 0.34 additional antennas per each 1% increment of network loading at BF, Uniform and CF ULD model, respectively. Similarly, adaptive system lowers number of antennas at different speeds as network loading decrease. These speed coefficients represent the slops of adaptive system at different ULD models. This result shows the significance of considering ULD models in adaptive antenna system design.

The relation between network loading and EE of fixed and adaptive antenna systems on BF, Uniform and CF ULD models is shown in Figure 3.4. Generally, All EE curves grow continuously as network approach its peak load at 100%. That is because both systems are basically designed to be on most energy efficient condition at maximum load. For fixed antennas system, the EE curves have negligible differences between ULD models except a slight lower value for BF ULD on peak load. The convergence of EE curves (blue lines) for fixed and adaptive systems on BF ULD model obviously reflects their meeting in number of antennas (black and red lines) at higher network loading in Figure 3.3. The EE of adaptive antenna system at Uniform and CF ULD models (red and green solid lines, respectively) is relatively higher their respective EE curves (red and green dashed lines) fixed antenna system. Adaptive antenna system at CF ULD model has the highest EE growth since it always operates lowest number of on antennas as network loading increase to peak conditions.

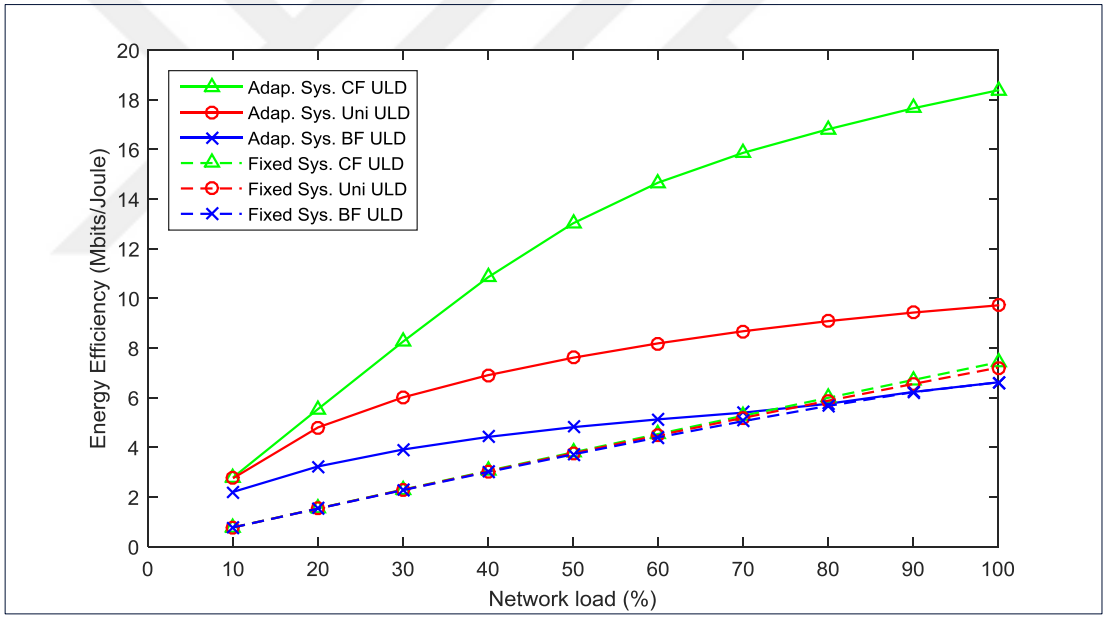

Figure 3.4. EE of fixed and adaptive antenna systems

In Figure 3.5, the average user-rates offered by fixed and adaptive antennas systems are shown by solid and dashed lines, respectively. Clearly, fixed antenna systems deliver better user-rates then adaptive systems. Fixed antenna system also provides different user-rates, though same number of antennas are employed in each one. This is simply due to the various ULD modes. As depicted, for fixed antenna systems the average user-rate of Uniform ULD model (red dashed line) is higher than BF (blue dashed line) and lower than CF ULD models (green dashed line). Similarly, for adaptive antenna systems the average user-rate of Uniform ULD model (red sold line) is higher than BF (blue solid line) and lower than CF ULD models (green solid line).

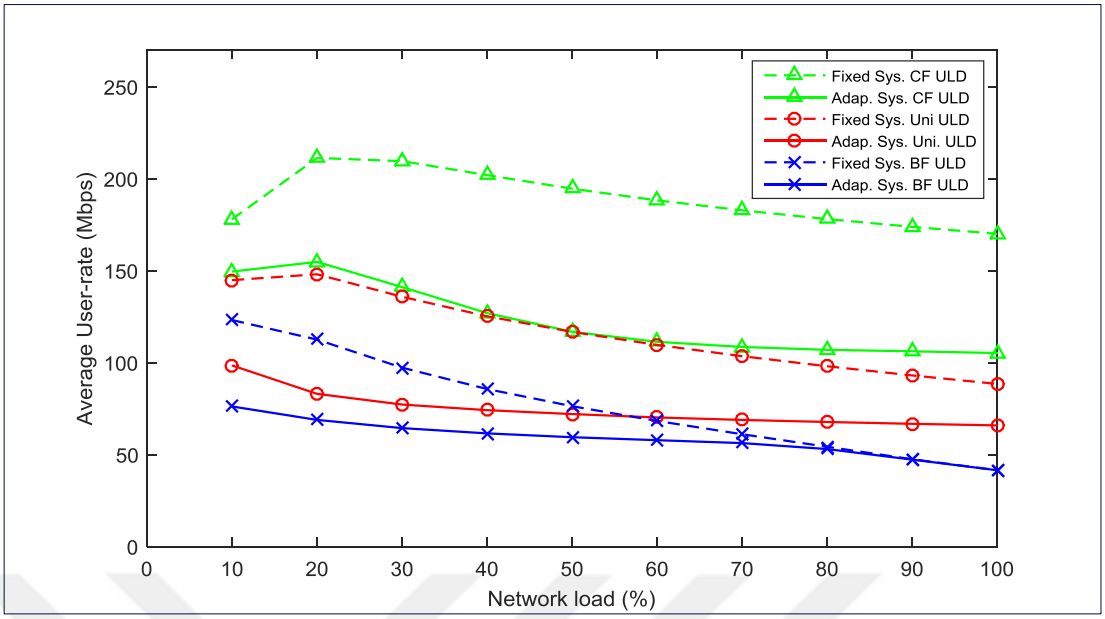

Figure 3.5. Average user-rate of fixed and adaptive antenna systems

3.3. EE Gain and User-Rate Loss Trade-Off

For the same ULD models used in Section 3.2 and illustrated in Table 3.1, we benchmark the fixed and adaptive antenna systems by relative metrics for EE gain and user-rate loss. EE gain as shown in Eq. (3.1) is simply the ratio of energy efficiency saving by adaptive system over the EE of conventional fixed antenna system. Similarly, the user-rate loss is the ratio of user-rate dropping by adaptive system over the user-rate of conventional fixed antenna system as shown in Eq. (3.2).

$$EE_{Gain} = \frac{EE_{Adaptive} - EE_{Fixed}}{EE_{Fixed}} \tag{3.1}$$

$$R_{Loss} = \frac{R_{Fixed} - EE_{Adaptive}}{EE_{Fixed}} \tag{3.2}$$

It is clear from Figure 3.6 that the obtainable EE gain for ULD models decreases at different trends as network loading increases, which is understandable as both systems are in the most energy-efficient state at peak network load. For the same reason, the user-rate losses decrease with varying speeds as the network loading increases as shown in Figure 3.7. Results show that the adaptive antenna system has a mean EE gain of 47%, 113% and 222% at the cost of 34%, 48% and 42% mean user-rate loss over the fixed antenna system for BF, uniform and CF ULD models, respectively.

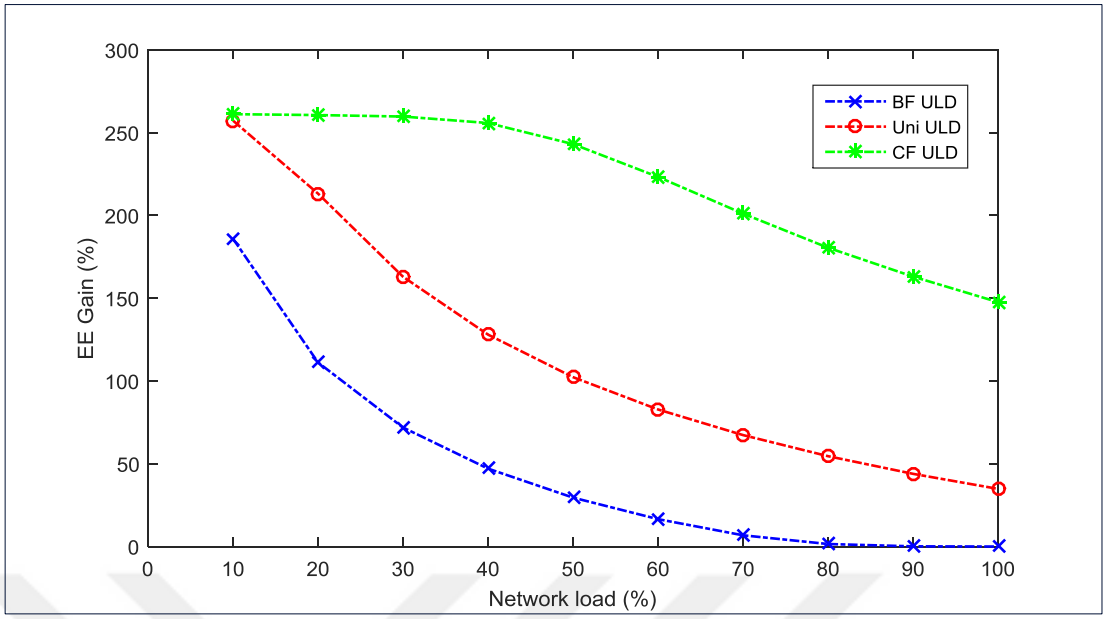

Figure 3.6. EE gain of adaptive antenna system on different ULD models

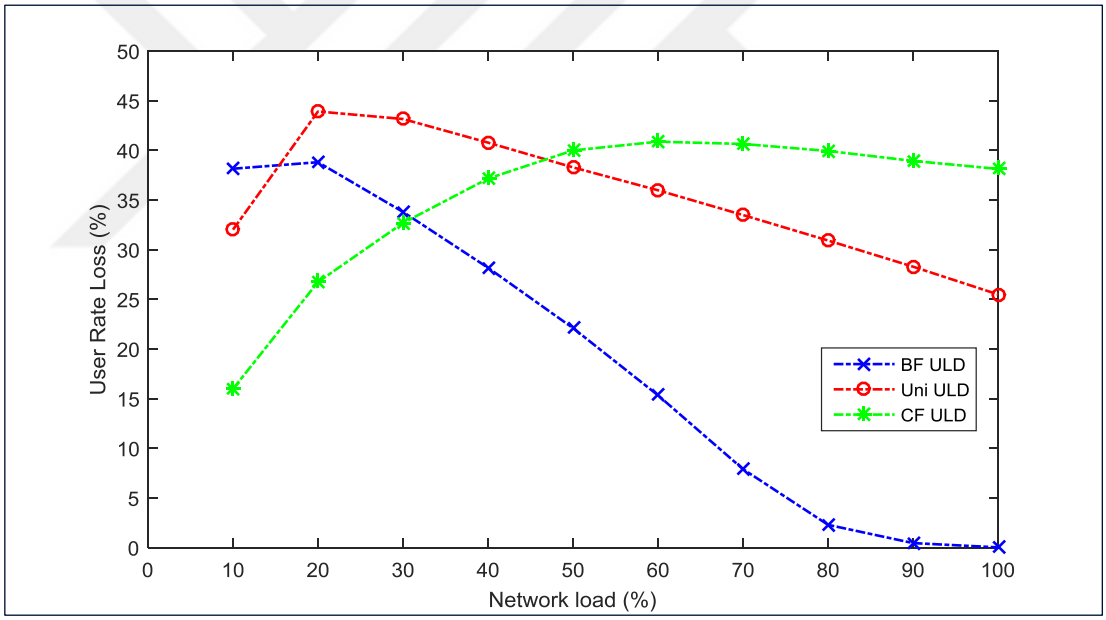

Figure 3.7. User-rate loss of adaptive antenna systems on different ULD modes

For the case when ULD is BF, the EE gain and user-rate loss diminish toward zero as the network approaches its 100% loading, where the configurations of adaptive and fixed antenna systems are going to be the same. The reason behind these results is the favorable propagation (aka the degree of freedom) in massive MIMO systems. In other words, when the ULD varies from BF to CF, the quality of radio conditions gets better, and the system obtains more channels that are independent. This variation can be exploited to reduce the number of antennas, thereby achieving a

more energy-efficient operation. The results obtained here emphasize the importance of considering ULD variation in dimensioning massive MIMO systems.

3.4. ULD Variation Effects on Fixed Antenna System Design

To examine the fixed antenna system design values (K_{max}, M_{max}), we form a ULD Model that varies from CF to BF by using the sets δ={400} and $\Gamma = \{(1,0), (0.9,0.1), (0.8,0.2) \ldots (0,1)\}$. This ULD model splits the cell coverage area into two regions, cell center area, enclosed by concentered circles of radii 35 m and 400 m, and cell boundary area, that lies from 400 m to cell border at radius of 500 m.

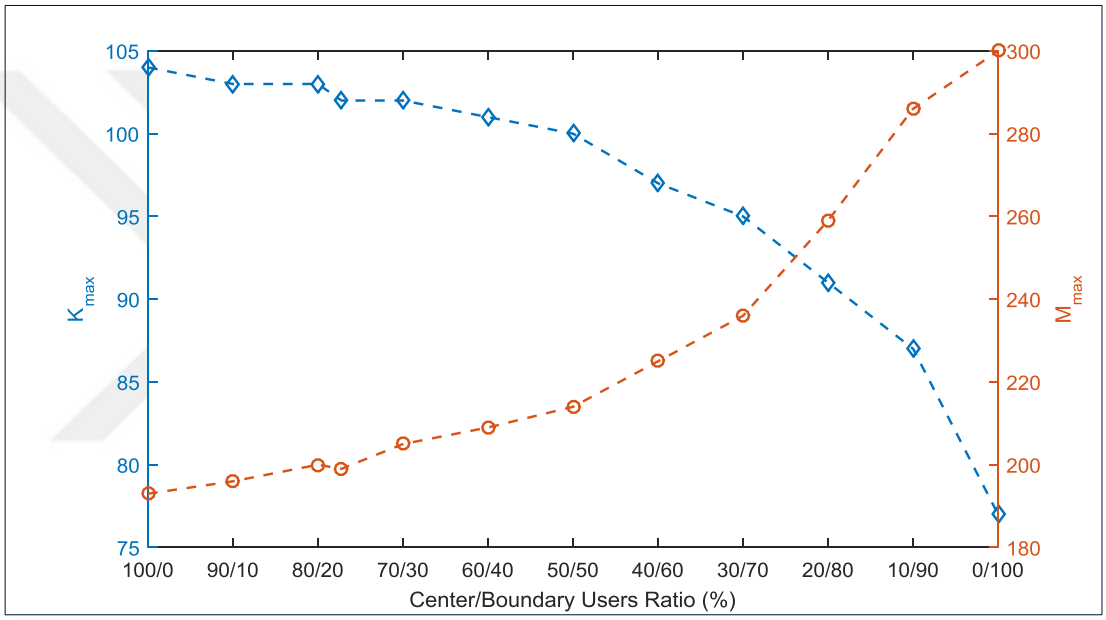

Figure 3.8. Fixed antenna system design parameters (K_{max}, M_{max}) versus center-to-boundary users' ratio

The maximum number of users that can be served, K_{max} decreases sharply and the corresponding number of antennas M_{max} increases rapidly as shown in Figure 3.8. In fact, these pairs of (K_{max}, M_{max}) correspond to the most energy-efficient operating points that describe the system capacity, (K_{max}) and BS resources requirements, (M_{max}). On the other hand, the user-rate at center and boundary regions (green and red curves) improves while the overall EE (blue curve) degrades as shown in Figure 3.9. Reversely, i.e. when ULD model transforms from BF to CF, the system capacity increases and BS resources requirements decreases while the user-rate at center and boundary regions degrades and the overall EE improves.

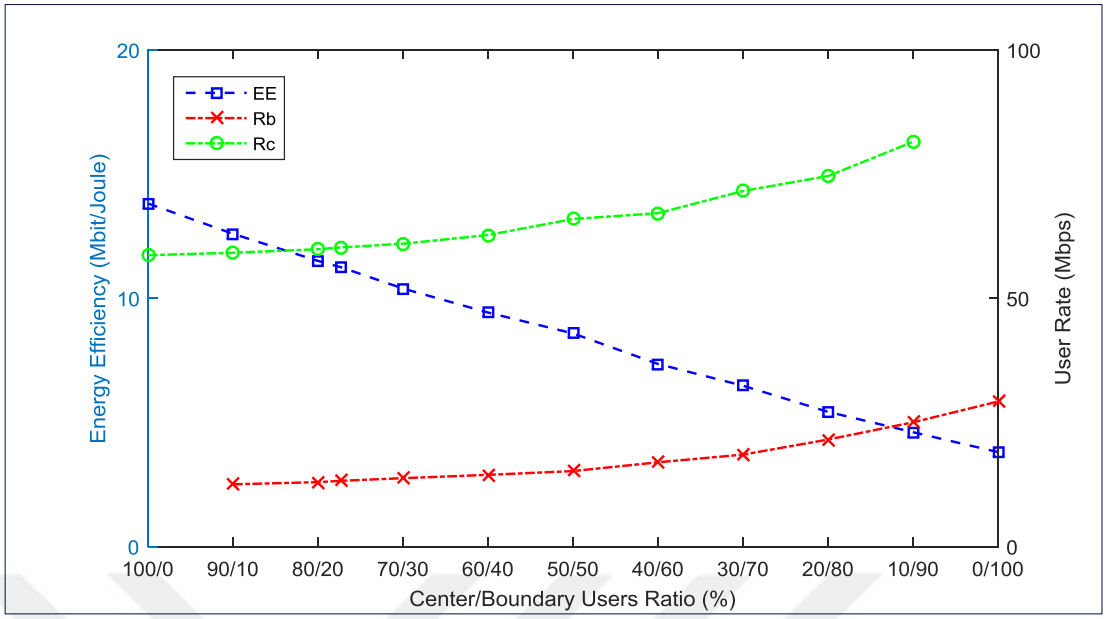

Figure 3.9. EE and average user-rate versus center-to-boundary users' ratio

3.5. Average Hourly Energy Consumption

As indicated in Section 3.3, adaptive system achieves more energy efficient operation by deactivating certain number of antennas at each network loading state. To capture the cost saving of such design, we need to analyze the effects of ULD variation in a time frame of 24 hours. Therefore, we examine the fixed and adaptive antenna systems on two ULD scenarios as illustrated in Figure 1.3. In both scenarios, the coverage area of cell under study is divided into three regions by the set of radii δ={200, 400} m to as presented in Figure 1.2. Then, we assign the weighting factors γ_A and γ_B as shown in Table 3.3. As is noticed from Figure 3.10, on average 144 of 227 and 108 of 232 antennas can be turned off during 24 hours for scenario-A and scenario-B, respectively. The results conclusively show that almost 60% and 50% of active antennas are deactivated every day at scenario-A and scenario-B, respectively, with the help of adaptive antenna system. Such a decrement is calculated to greatly conserve the total network energy consumption and consequently, reduce operator's OpEx. An appropriate metric to evaluate the amount of energy savings is the AEC as in Eq. (1.9). As demonstrated in Figure 3.11, approximately 51% and 36% of average consumed energy of fixed antenna system can be saved at scenarios A and B, respectively, by adopting adaptive antenna allocation strategy that copes with ULD variation and network loading simultaneously.

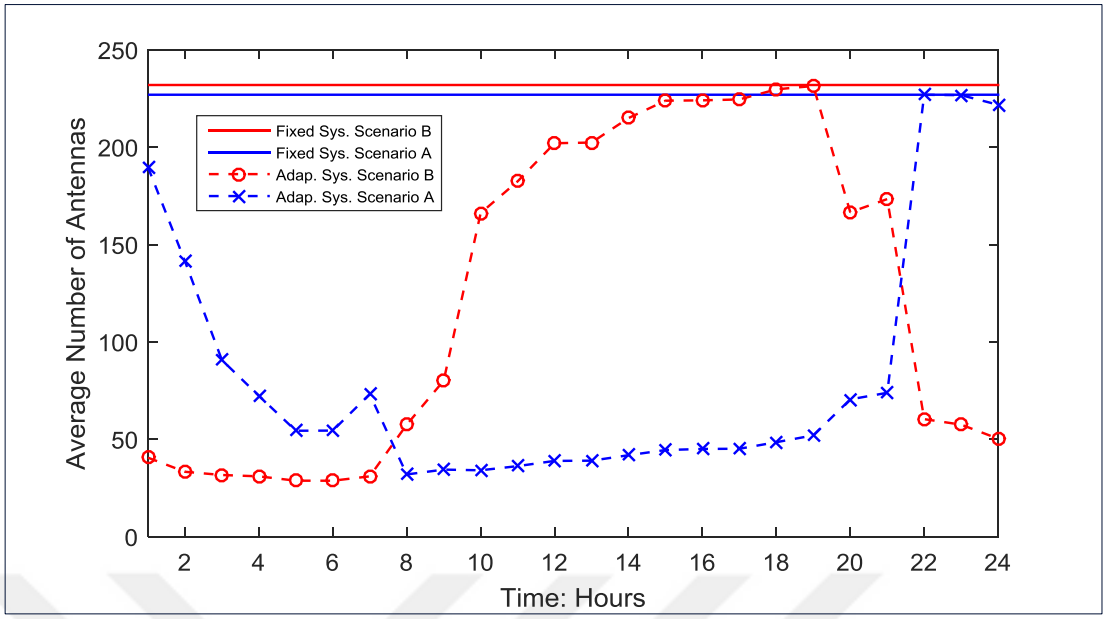

Figure 3.10. Number of Antennas vs. Hours of the day

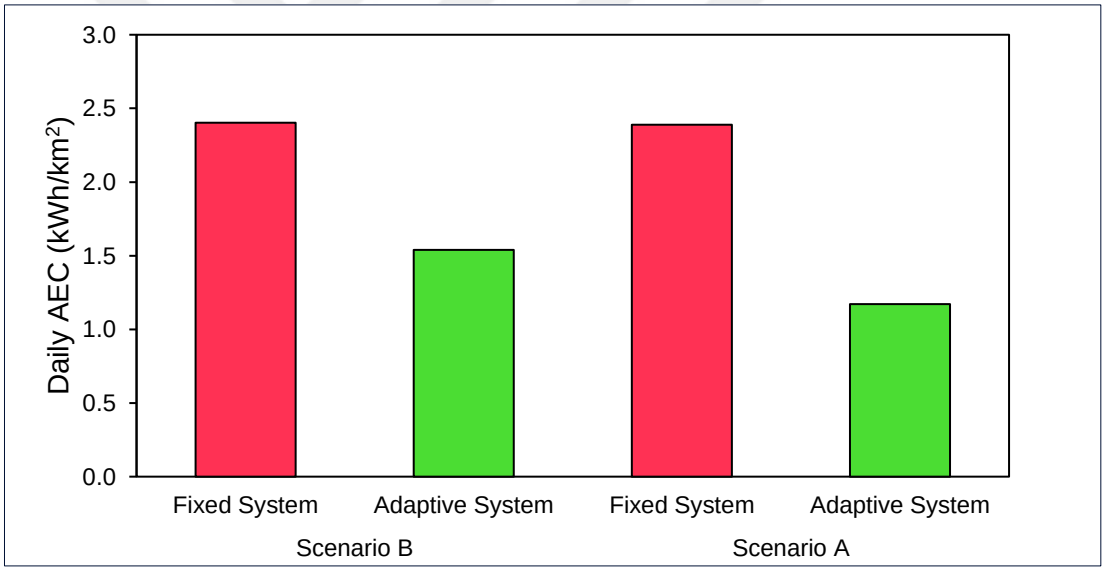

Figure 3.11. Energy consumption of fixed and adaptive systems

Table 3.3. Daily ULD scenarios

		Time (Hour in a day)				
		01 – 07	08 – 09	10 – 19	20 – 21	22 – 24
Scenarios	γ_A	(0.1, 0.2, 0.7)	(0.6, 0.2, 0.2)	(0.8, 0.1, 0.1)	(0.6, 0.2, 0.2)	(0.1, 0.2, 0.7)
	γ_B	(0.7, 0.2, 0.1)	(0.2, 0.2, 0.6)	(0.1, 0.1, 0.8)	(0.2, 0.2, 0.6)	(0.7, 0.2, 0.1)

3.6. Number of Antennas for BS GDR Level

As we observed in Figure 3.3, adaptive system hires additional 1.3 antennas at each increment of 1% of network loading on Uniform ULD model. The ultimate purpose of that design was to ensure system operating on maximum possible EE state regardless of user-rate loss. So, the BS was offering a best-effort user-rate. In this section, we apply algorithm (b) shown in Figure 2.2 to control user-rate loss at BS level and to retain EE somehow on optimal standing. The QoS target is set to keep a guaranteed data rate (GDR) at BS whatever variations in network loading or ULD model. As video and audio traffic have around 74% share of mobile data traffic forecast [20], we assumed mobile applications are split into two main categories, streaming and non-streaming applications. Then, we assume four scenarios for ratio of streaming applications that can considered as different user traffic profiles. By applying Eq.(1.5), we get four amounts of average user-rate at BS level as shown in Table 3.4.

Table 3.4. Mobile data traffic forecast [18-20]

<table>
<tr><td rowspan="3">BH Users</td><td rowspan="3">Activity factor</td><td rowspan="2" colspan="2">Connected Users Split per Device Category</td><td rowspan="2" colspan="2">Mobile Data Split per App Category (GB/month)</td><td colspan="4">Streaming Application Ratio</td></tr>
<tr><td>25%</td><td>50%</td><td>75%</td><td>100%</td></tr>
<tr><td>Smartphones</td><td>95%</td><td>Streaming traffic</td><td>38,1</td><td colspan="4">Average User-rate (Mbps)</td></tr>
<tr><td>96</td><td>10%</td><td>Mobile PCs, Tablets & Routers</td><td>5%</td><td>Non-streaming Traffic</td><td>4,8</td><td>43</td><td>71</td><td>98</td><td>126</td></tr>
</table>

For the sake of clarity, in below we present the simulation results for Uniform ULD model only. The results for BF and CF ULD models are presented in Appendix-A. The average number of antennas in Figure 3.12 increases noticeably as BS GDR level goes up. As can be seen also, the upper limit is the number of antenna at fixed system. The red curve belongs to adaptive antenna system for maximum EE and best-effort user rate as resulted by Figure 2.1. For 43 Mbps GDR level, the average number of antennas has the same values over all network loads as in red curve. Back to Figure 3.5, the average user rate for Uniform ULD model is always above the 43 Mbps GDR level. This means that adaptive system set number of antennas driven by Figure 2.1 as lower limits to maintain optimum EE whenever possible. As result of that, red and green curves are exchangeable in near upcoming analysis.

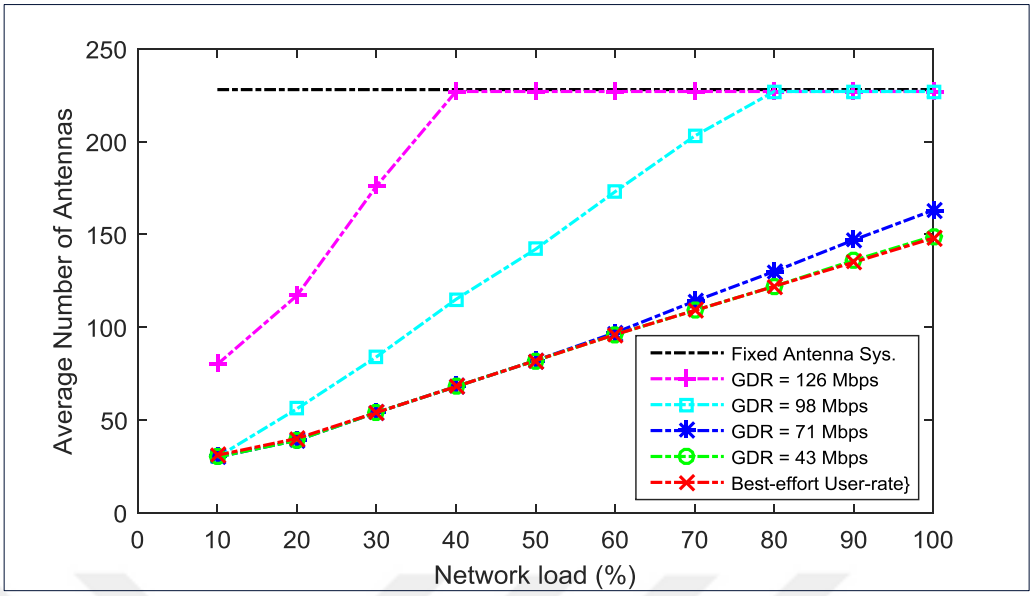

Figure 3.12. Number of antennas for Uniform ULD at various BS GDR levels

The BS average user-rates that come out of GDR BS levels, are displayed in Figure 3.13. For 128 and 98 Mbps GDR levels, the adaptive system provides BS average user-rates (magenta and cyan dashed lines) lower than GDR level when network loading higher than 40% and 80%, respectively. This is due to the fact, number of antenna cannot go beyond fixed system design as already shown in Figure 3.12. At 71 Mbps GDR level, the BS average user rate (blue curve) starts to deviate from best effort user-rate (green line) at network loading 60% and upwards. This illustrates how adaptive system activates additional antennas to recover user-rate loss when BS average user-rate drops below GDR level.

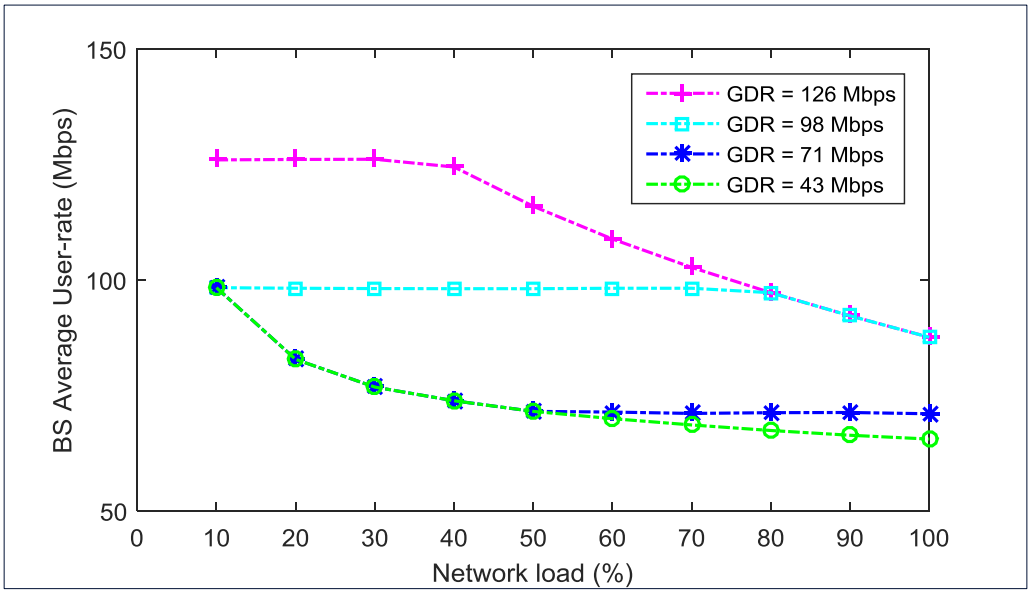

Figure 3.13. BS average user-rate for Uniform ULD at various BS GDR levels

3.7. Number of Antennas at User Satisfaction Level

Before we move to analysis of algorithm (b) shown in Figure 2.2, it is worthwhile to present the percent of users getting data rate equal or higher than GDR levels as already found in Section 3.6 . As can be seen form Figure 3.14, the ratio of users satisfying BS GDR levels decreases steadily as network loading approach 100%. To control such decrement, we introduce the 2nd QoS requirement to maintain certain ratio of users gets GDR level as shown in Table 3.5. The considered ratios are aligned with results in Figure 3.14, to obtain meaningful results.

Table 3.5. User satisfaction scenarios

Scenario	GDR Level (Mbps)	Percent of users satisfying GDR level
1	43	80%
2	71	60%
3	98	40%
4	126	20%

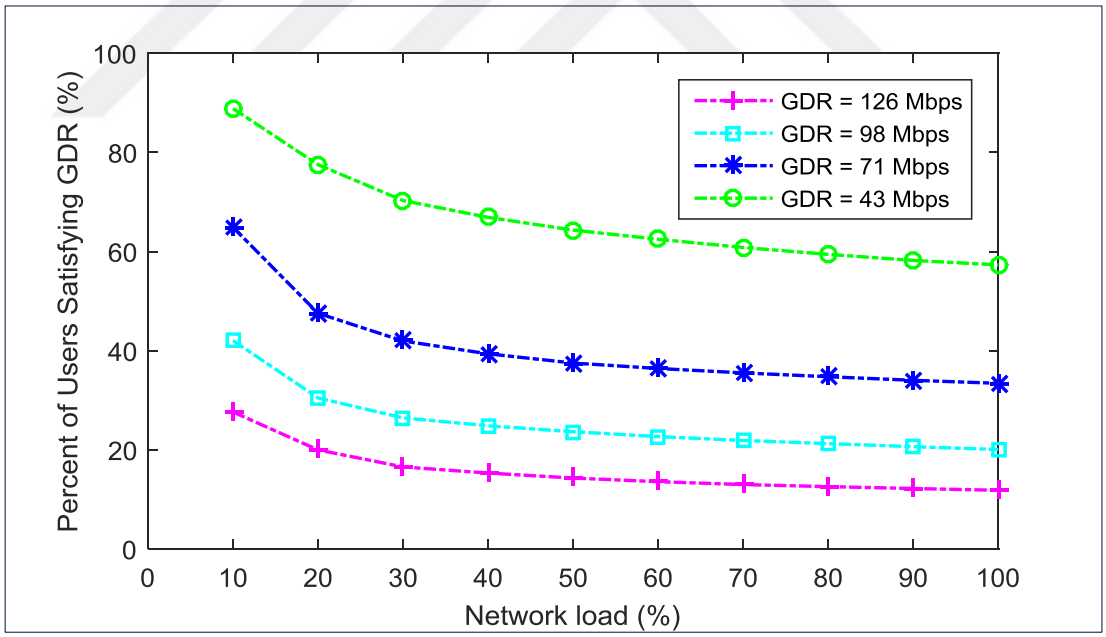

Figure 3.14. Percent of users satisfying GDR levels at Uniform ULD

As shown in Figure 3.15, the average number of antennas (all curves) this time is dimensioned to maintain a ratio of users exceeding the GDR level. Aside from pervious analysis for Figure 3.12, number of antennas for scenario 4 (20% of users get 126 Mbps GDR or more) in magenta line is lower than number of antennas for scenario 3 (40% of users get 98 Mbps GDR or more) in cyan line.

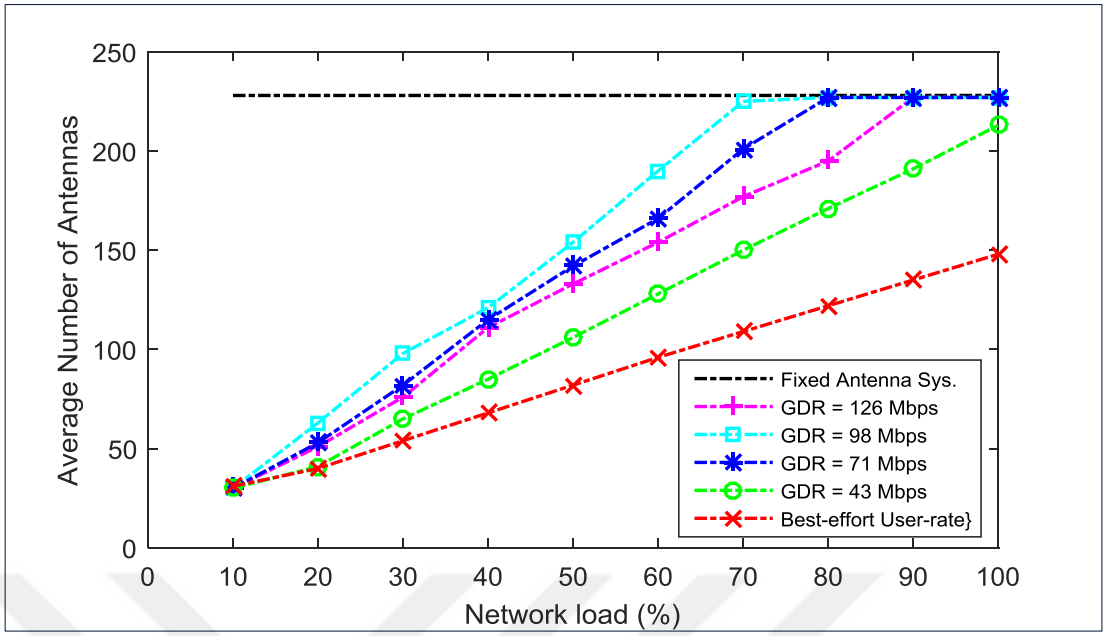

Figure 3.15. Number of antennas for Uniform ULD at various user satisfaction levels

In this context, the BS average user-rates as shown in Figure 3.16 do not evaluate adaptive system performance as they represent the user-rate for overall users in cell under study while Algorithm (b) shown in Figure 2.2 enhance the user-rate for certain portion of users. In Figure 3.17, we can see how users stratification maintained up to certain levels over all network loads in accordance to QoS requirements in Table 3.5.

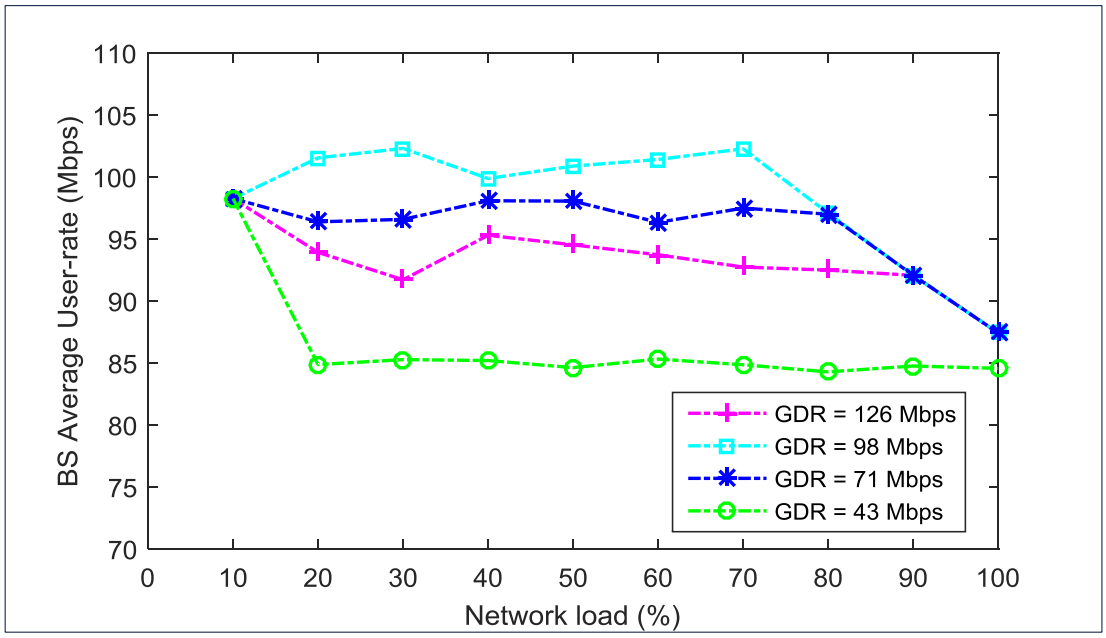

Figure 3.16. BS average user-rate for Uniform ULD at various user satisfaction levels

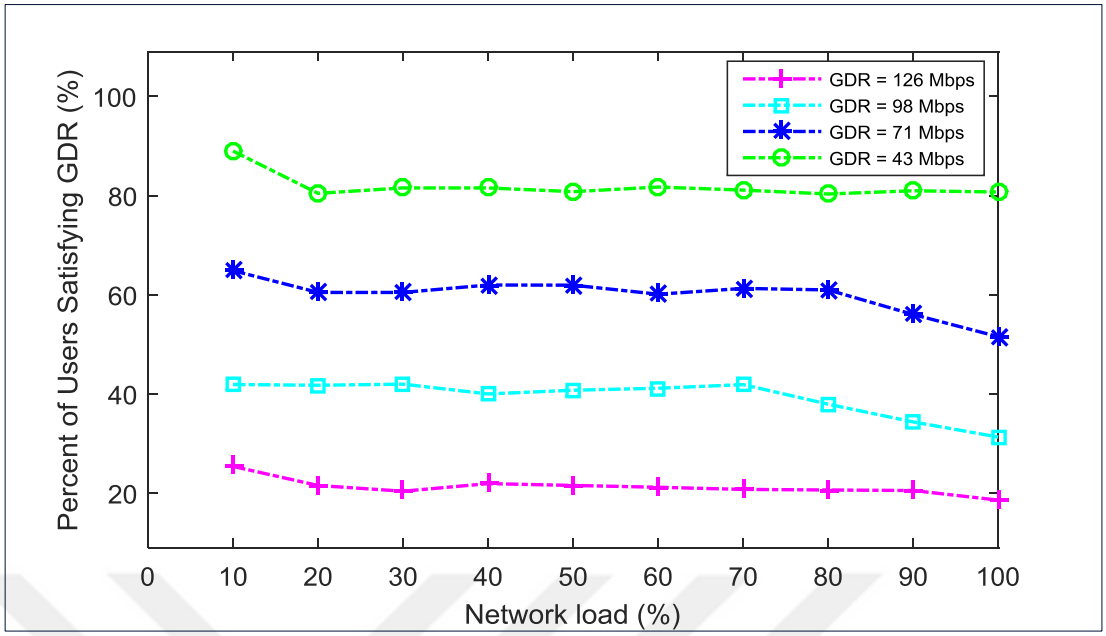

Figure 3.17. Guaranteed percent of users satisfying GDR levels at Uniform ULD

4.CONCLUSION

In this study, we investigate the effects of daily ULD variation on the energy efficiency of a massive MIMO system. For that purpose, we proposed several ULD models and examined the optimum number of antennas that maximizes EE in all user states under different cell loading conditions. These models divide the hexagonal cell into certain number of areas and distribute users hourly inside each one according to statistical ULD model. Each BS is modelled as an M/G/m/m queue, where user steady state probabilities are distributed with respect to average user-rates. The cells are assumed symmetrical in all aspects. Therefore, the analysis is carried out over the cell under study only by using EE optimization algorithm to obtain the optimal number of antennas that maximizes EE at each user state at the cost of rate loss. We have found that the considerable impact on optimal antenna allocation is associated with ULD variation rather than daily load profile and the relation between the number of antennas and the number of users is almost linear. To make a fair comparison, we assume a baseline system that operates by a fixed number of antennas that corresponds to the highest EE at minimum center-to-boundary users' ratio and, concurrently, maximal cell load. For dynamic ULD models, adaptive antenna systems can achieve 47%, 113%, and 222% EE gain over fixed ones at the cost of 19%, 35% and 35% rate losses for BF, Uniform, and CF models, respectively. Since the analysis was carried out over a cell load range of 10-100% while 34% of daily load profile hours are below half-cell loading condition, these results show that ULD models significantly outperform the baseline system. In a 24-hour analysis framework, the simulation results show that one third of the active antennas can be turned off and consequently up to 50% of consumed energy can be conserved after adopting cell load adaptive antenna system with ULD. For fairness, this work has been carried out by modelling ULD in a reasonable way and actual users may not follow proposed ULD models. In addition, the symmetrical condition may not hold for a coverage area of radius 4 km. Nevertheless, the same procedures can be carried under real conditions if a detailed radio description and traffic statistics are provided.

APPENDICES

Appendix A: Adaptive Antenna System at BF and CF ULD Models

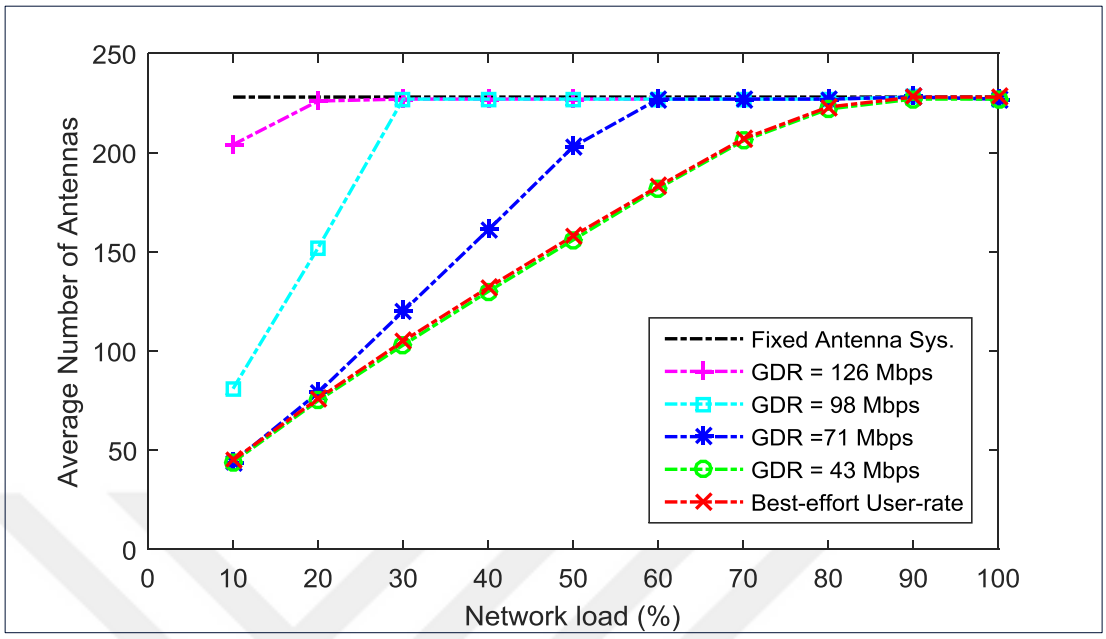

Figure 4.1. Number of antennas for BF ULD at various BS GDR levels

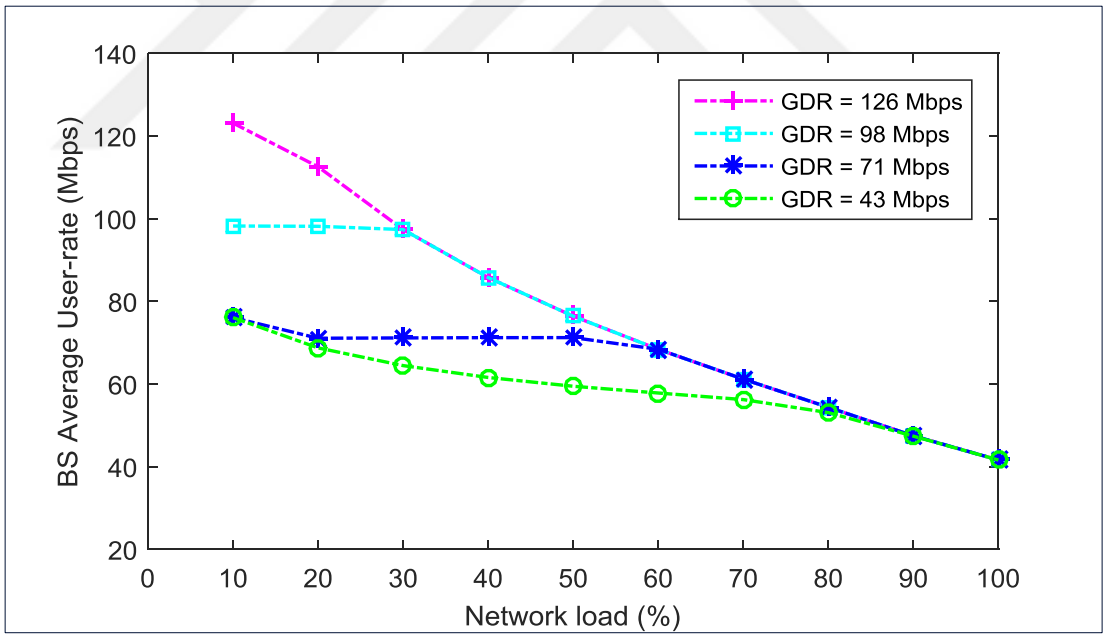

Figure 4.2. BS average user-rate for BF ULD at various BS GDR levels

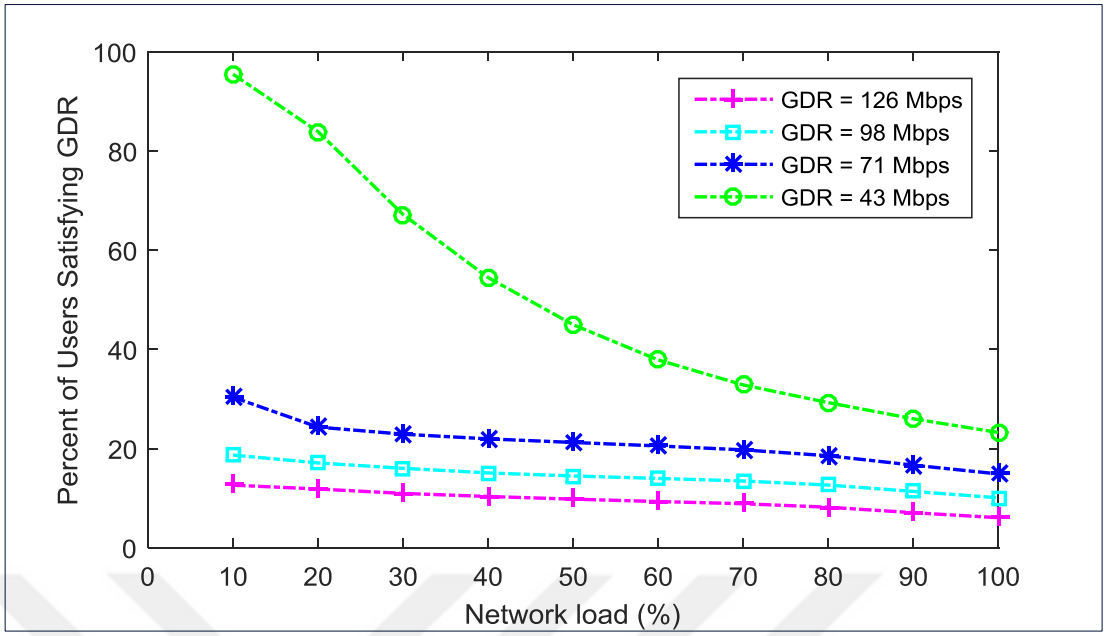

Figure 4.3. Percent of users satisfying GDR levels at BF ULD

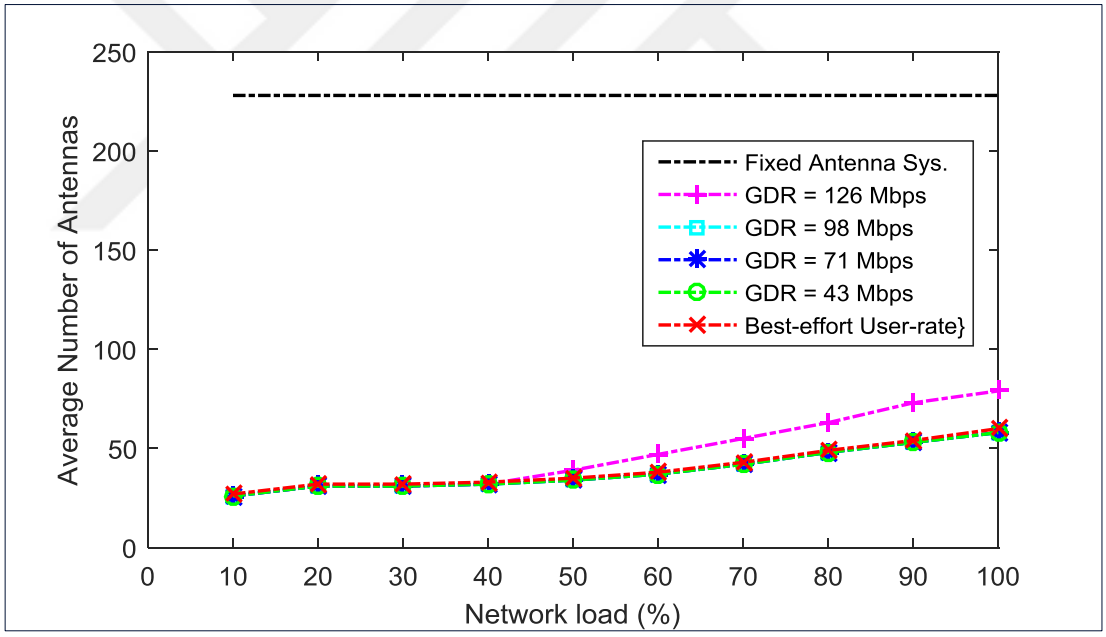

Figure 4.4. Number of antennas for CF ULD at various BS GDR levels

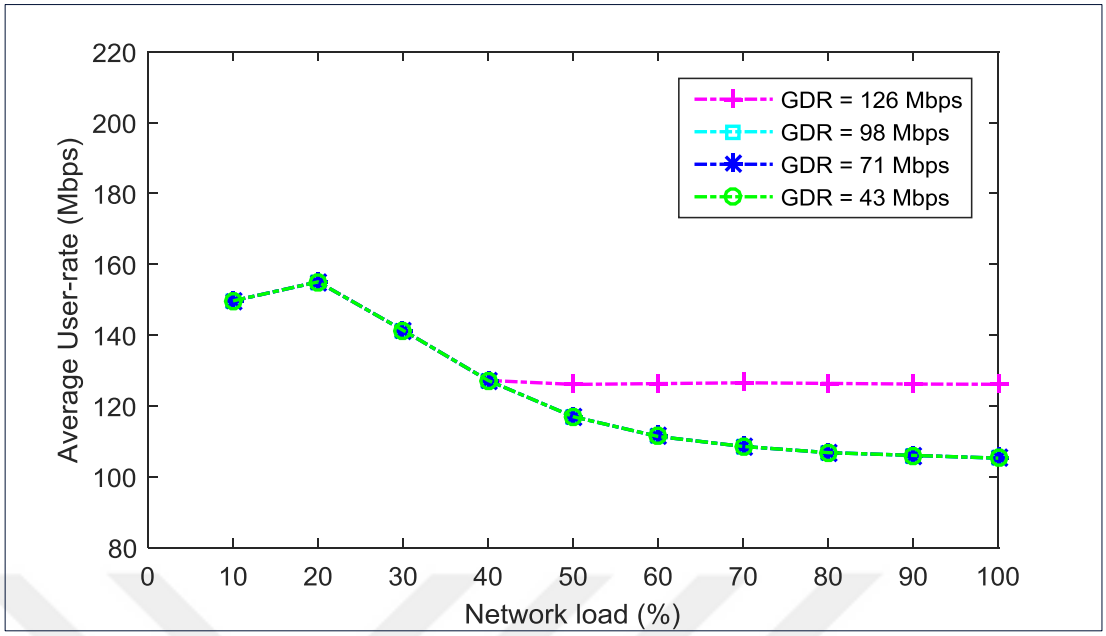

Figure 4.5. Average user-rate for CF ULD at various BS GDR levels

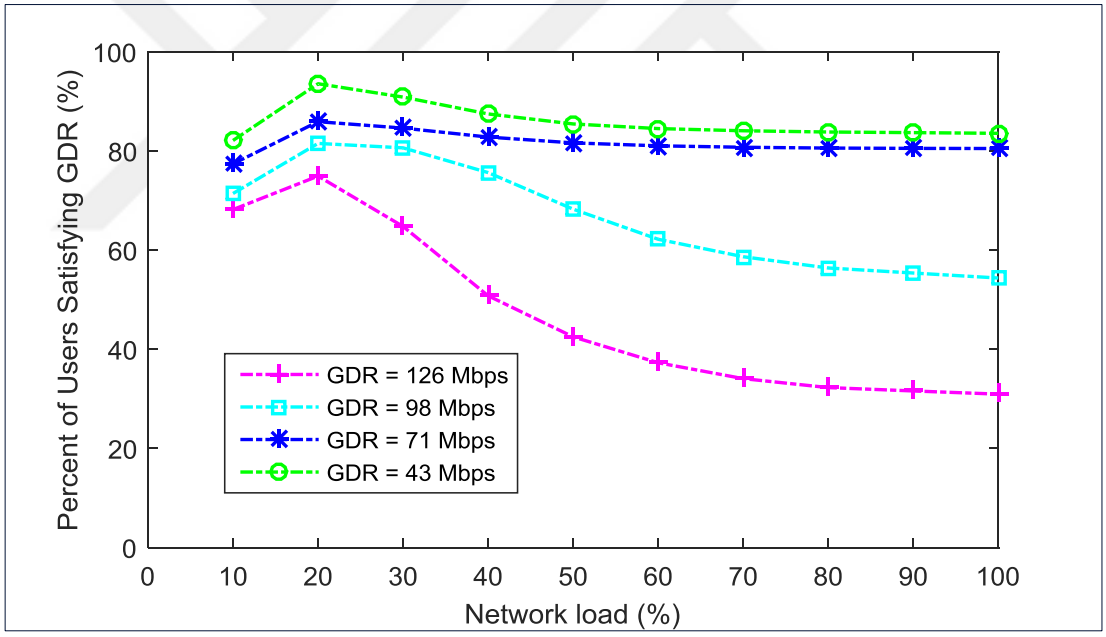

Figure 4.6. Percent of users satisfying GDR levels at CF ULD

REFERENCES

[1] Dahlman et al., 5G Wireless Access: Requirements and Realization, *IEEE Commun. Mag.*, 2014, **52** (12), 42–47.

[2] Wang et al. C.-X., Cellular Architecture and Key Technologies for 5G Wireless Communication Networks, *IEEE Commun. Mag.*, 2014, **52** (2),122–130.

[3] Osseiran A, Monserrat J. F., Marsch P., et al., *5G Mobile and Wireless Communications Technology*, Cambridge University Press, United Kingdom, 2016.

[4] Le L. B., Enabling 5G Mobile Wireless Technologies, *EURASIP J. Wireless Commun. Netw.*, 2015, **2015** (1), 1–14.

[5] Marinello J. C., Abrão T., Pilot Distribution Optimization in Multi-Cellular Large Scale MIMO Systems, *AEU - International Journal of Electronics and Communications*, 2016, **70** (8), 1094-1103.

[6] Sure P., Bhuma C. M., A Pilot Aided Channel Estimator Using DFT Based Time Interpolator for Massive MIMO-OFDM Systems, *AEU - International Journal of Electronics and Communications*, 2015, **69** (1), 321-327.

[7] Larsson E. G., Edfors O., Tufvesson F., Marzetta T. L., Massive MIMO for Next Generation Wireless Systems, *IEEE Commun. Mag.*, 2014, **52** (2), 186-195.

[8] Marzetta T. L., Noncooperative Cellular Wireless with Unlimited Numbers of Base Station Antennas, *IEEE Trans. Wireless Commun.*, 2010, **9** (11), 3590-3600.

[9] Ngo H. Q., Larsson E. G., Marzetta T. L., Energy and Spectral Efficiency of very Large Multiuser MIMO Systems, *IEEE Trans. Commun*. 2013, **61** (4), 1436–1449.

[10] Björnson E., Sanguinetti L., Hoydis J., Debbah M., Designing Multi-User MIMO for Energy Efficiency: When is Massive MIMO the Answer?, *2014 IEEE Wireless Commun. and Networking Conference* (WCNC), Istanbul, Turkey, April 6–9, 2014.

[11] Hasan Z., Boostanimehr H., Bhargava V. K., Green Cellular Networks: A Survey, Some Research Issue and Challenges, *IEEE Commun. Surveys & Tutorials,* 2011, **13** (4), 524–540.

[12] Han C., Harrold T., et al., Green Radio: Radio Technique to Enable Energy-Efficient Wireless Networks, *IEEE Commun. Mag.*, 2011, **49** (6), 46–54.

[13] Hossain M. M. A., Çavdar C., Björnson E., Jäntti R., Energy-Efficient Load-Adaptive Massive MIMO, *2015 IEEE Globecom Workshops (GC Wkshps)*, 2015.

[14] Karlsson A., et al., Energy-Efficient 5G Deployment in Rural Areas, *IEEE WiMob*, New York, USA, Oct. 17-19, 2016.

[15] Thakur R., Singh R., Murthy C. S. R., An Energy Efficient Framework for User Association and Power Allocation in HetNets with Interference and Rate-loss Constraints, *Computer Communications*, 2016 **94**, 57-71.

[16] Chen Y., Zhang S., Xu S., Li G., Fundamental Trade-Offs on Green Wireless Networks, *IEEE Commun. Mag.*, 2011, **49** (6), 30–37.

[17] Björnson E., Sanguinetti L., Hoydis J., Debbah M., Optimal Design of Energy-Efficient Multi-User MIMO Systems: Is Massive MIMO The Answer?, *IEEE Trans. Wireless Commun.*, 2015, **4** (6), 3059–3075.

[18] Auer G. et al., D2.3: Energy Efficiency Analysis of the Reference Systems, Areas of Improvements and Target Breakdown, Energy Aware Radio and Network Technologies (EARTH) INFSO-ICT-247733, ver. 2.0, 2012. Available: http://www.ict-earth.eu/, [Accessed Date: Mar 17, 2018].

[19] ETSI ES 202 706-1, Environmental Engineering (EE) Metrics and Measurement Method for Energy Efficiency of Wireless Access Network Equipment, *European Telecommunications Standards Institute*, Oct. 2016. Available: http://www.etsi.org/ [Accessed Date: Mar 17, 2018].

[20] AMERICAN TIME USE SURVEY — 2016 RESULTS. Available: https://www.bls.gov/news.release/pdf/atus.pdf [Accessed Date: Mar 17, 2018]

[21] Ericsson Traffic Exploration Tool. Available: https://www.ericsson.com/TET/ [Accessed Date: Mar 17, 2018].

[22] Nokia Bell Labs, Who will satisfy the desire to consume?, (15 Nov. 2016) Available: https://www.bell-labs.com/var/articles/bell-labs-mobility-report/ [Accessed Date: Mar 17, 2018]

[23] Huawei Wireless X Labs, The Future of Mobile Broadband. How Mobile Operators Can Deliver the Connected Life between Now and 2025?, (Feb. 2017), Available: http://www.huawei.com , [Accessed Date: Mar. 17, 2018].

[24] Hossain M. M. A., Koufos K., Jäntti R., Minimum-Energy Power and Rate Control for Fair Scheduling in the Cellular Downlink under Flow Level Delay Constraint, *IEEE Trans. Wireless Commun.*, 2013, **12** (7), 3253–3263.

[25] Hossain M. M. A., R. Jäntti, Impact of efficient power amplifiers in wireless access, *2011 IEEE Online Conference on Green Communications*, 2011, New York, NY, 36-40.

[26] Chenand L., Chen W., Wang B., Zhang X., Chen H., Yang D., System-level Simulation Methodology and Platform for Mobile Cellular Systems, *IEEE Communications Magazine*, 2011, **49** (7), 148-155.

PUBLICATIONS AND WORKS

[1] **Abuibaid M.A.**, Aldırmaz Çolak S., Energy-efficient massive MIMO system: Exploiting user location distribution variation, *AEU-International Journal of Electronics and Communications,* 2017, **72**, 17-25.

[2] **Abuibaid M.A.**, Aldırmaz Çolak S., Optimum Number of Antennas for Energy Efficiency versus User Location in Massive MIMO Systems, *2017 25th Signal Processing and Communications Applications Conference (SIU)*, 2017, doi:10.1109/siu.2017.7960155.

BIOGRAPHY

Mohammed A.A. ABUIBAID was born in Rafah, Palestine, in 1990. He received a B.E. degree in Telecommunication Engineering from An-Najah National University, Nablus, Palestine, in 2013. On the same year, he joined Wataniya Mobile as Radio Network Planning & Optimization engineer. In 2015, he joined Department of Electronic and Communication Engineering at Kocaeli University as a researcher in the field of Massive MIMO design. In 2017, he joined Nokia Solutions and Networks as a Technical Configuration Consultant for Nokia Radio Portfolio.